Pyridine Containing Aromatic Polyether Membranes

5

Joannis K. Kallitsis, Aikaterini K. Andreopoulou, Maria Daletou, and Stylianos Neophytides

5.1 Introduction

A lot of scientific effort has been devoted to the design and development of the different components (catalysts, membranes) of the polymer electrolyte membrane (PEM) fuel cells (FC) s resulting in a real explosion of field electricity production from hydrogen. This combined with the drastic increase of the natural gas reserves and availability, open new ways of consideration for the decentralized electricity production. One of the main ideas is the use of natural gas for hydrogen production that will be subsequently used as feed for devices that can effectively and with high yield produce energy. In this case the high temperature operation of the PEM FCs can offer a unique solution since even hydrogen containing impurities can be used. The electricity and thermal energy cogeneration is one case where the total energy efficiency can be increased up to 80–90 %. Another option is the operation at temperatures above 200 °C, so that the high temperature MEA is combined with a methanol reformer, thus enabling the use of liquid fuels like methanol. A further outcome of the high temperature operation is the use of such membranes and membrane electrode assemblies (MEAs) as electrochemical membrane reactors for the hydrogen purification instead of the palladium membranes used up to now. Based on the above considerations, from our perspective it was crucial to substantially increase the operation temperature for HT PEM FCs well above 200 °C. In the following chapter, we describe in detail our efforts and final outcome for the 1000 h stable operation of HT-PEMFCs at temperatures up to 210 °C.

5.2 Synthesis of Linear Aromatic Polyethers Containing Main Chain Pyridine Units

The idea to combine basic polymeric backbones with strong acids resulting in ionic conductive composites has been successfully demonstrated by the Savinell group back in 1995 [1]. This revolutionary approach combined the good mechanical properties of a rigid polymeric backbone with the acid absorption through the interaction with the basic backbone units creating clusters of acid molecules, thus enabling the proton transport. A number of studies were devoted to the understanding of the conduction process [2]. Despite the fact

J.K. Kallitsis (✉) • A.K. Andreopoulou
Department of Chemistry, University of Patras, Rio-Patras 26504, Greece

Foundation for Research and Technology Hellas/Institute of Chemical Engineering Sciences (FORTH/ICE-HT), Patras 26504, Greece
e-mail: j.kallitsis@upatras.gr

M. Daletou • S. Neophytides
Foundation for Research and Technology Hellas/Institute of Chemical Engineering Sciences (FORTH/ICE-HT), Patras 26504, Greece

Q. Li et al. (eds.), *High Temperature Polymer Electrolyte Membrane Fuel Cells*,
DOI 10.1007/978-3-319-17082-4_5

that this idea was demonstrated for quite a long time, the initial polymer polybenzimidazole (PBI) remained for long time as the only solution. Later on, relative structures like the poly (2,5-benzimidazole) AB-PBI were also used doped with phosphoric acid [3–5] and most recently structures combining the imidazole units with pyridine ones were also developed [6].

The idea to use the pyridine units as basic moieties in a rigid aromatic polymer was firstly demonstrated by our group in 2003 [7]. In this first approach, despite the use of the pyridine main chain units, phenyl phosphinoxide moieties were also included in the polymer structure both to improve solubility and to create more interaction sites with the phosphoric acid doping agent. New monomers were prepared using palladium-mediated cross coupling of 2,5- or 2,6-dibromopyridine with a properly protected boronic acid [8]. Scheme 5.1 presents the reaction employed for the preparation of the respective diols. 2,5-Dibromopyridine and 2,6-dibromopyridine were reacted via Suzuki coupling with the tetrahydropyranyloxy THP protected hydroxyphenylboronic acid producing the corresponding THP-end protected monomers in gram-scale quantities. The removal of the THP moieties was performed under acidic conditions. High-temperature polymerization of the synthesized diols with phosphinoxide difluoride was employed for various reaction times. **Homopolymers I** and **II** showed solubility in common organic solvents such as $CHCl_3$, allowing for their detailed characterization.

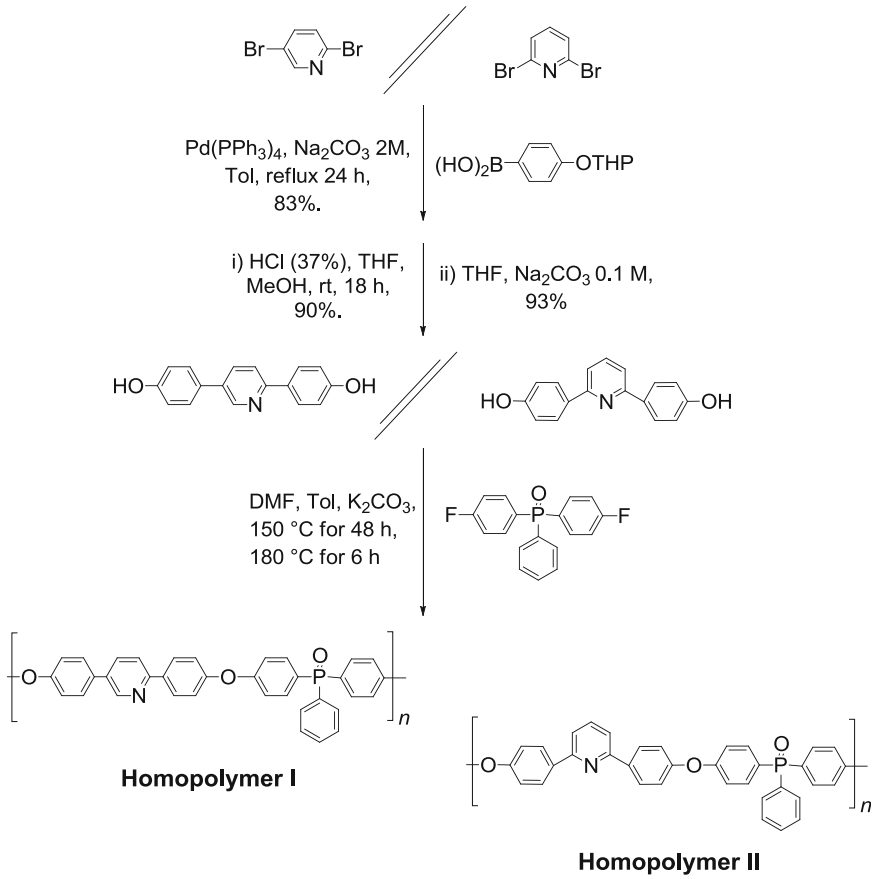

Scheme 5.1 Reaction sequences employed for the preparation of 2,5-bis(4-hydroxyphenyl)pyridine and 2,6-bis (4-hydroxyphenyl)pyridine and their polymerization with bis(4-fluorophenyl)phenylphosphine oxide producing **Homopolymers I** and **II**, respectively. Reproduced from [7] with permission of the American Chemical Society

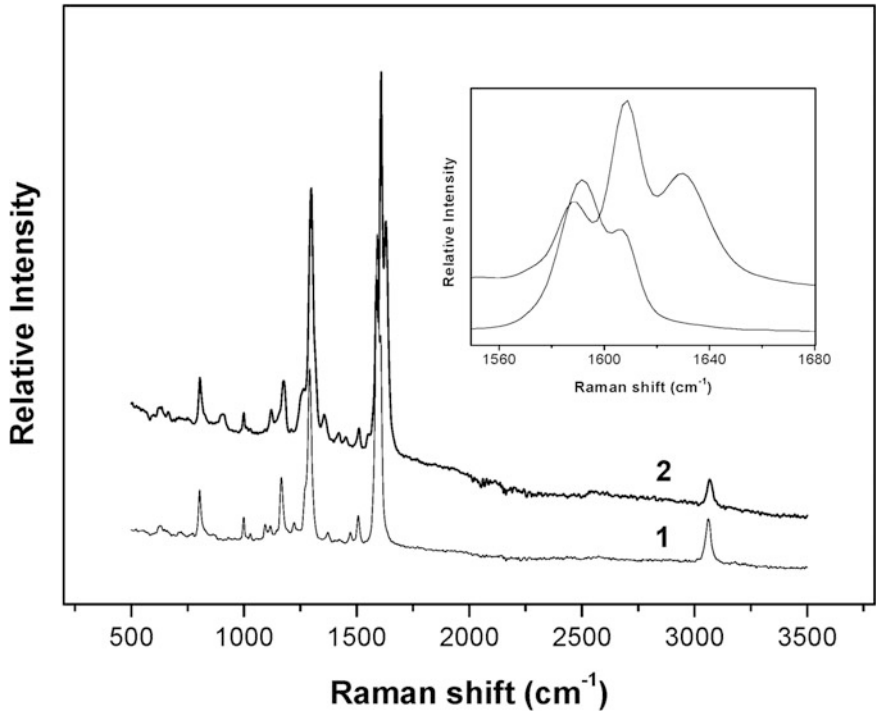

Fig. 5.1 FT-Raman spectra of **Homopolymer I** before (***1***) and after (***2***) doping with H_3PO_4 85 %. *Inset*: 1550–1680 cm^{-1} region. Reproduced from [7] with permission of the American Chemical Society

Materials with excellent film-forming properties were obtained. Structural characterization confirmed the expected structure and their physicochemical characterization showed high mechanical and thermal stability. The protonation of the membrane after its exposure to a strong acid could affect its thermal stability, so the thermogravimetric results before and after treatment with H_3PO_4 for 1000 h showed that the membrane is hydrolytically stable. During this study the interaction of the pyridine units with phosphoric acid was demonstrated using Raman by the shift of the peak at 1600 cm^{-1} of the pyridine to 1630 cm^{-1} after protonation, which is attributed to the C=N vibration of the protonated ring (Fig. 5.1). Also the phosphoric acid uptake of these polymers was very high providing the necessary conditions for high ionic conductivity.

However these homopolymers faced two main problems. Limitations in obtaining high molecular weights since insoluble materials were produced when the number average molecular weight (Mn) exceeded 50,000 and extensive plasticization from phosphoric acid of the low Mn materials. Indeed, a systematic investigation [9] showed that homopolymers containing the 2.5-bis(4-hydroxyphenyl) pyridine, which was the key monomer combining the presence of the pyridine units in the main chain and having the polymerizable phenols in *para* position to avoid sterical hindrance, faced solubility limitations. In order to understand the nature of this insolubility a kinetic study of the polymerization (Fig. 5.2) was performed, which showed that as soon as a critical molecular weight value is reached, the polymer becomes partially soluble and finally insoluble.

In order to overcome this problem two routes were chosen. The first was to incorporate solubilizing side chain substituents along the polymeric main chain. The second was to use small amounts of other comonomers that would enhance solubility. The target of both routes was to achieve higher molecular weights while increasing the solubility of the final homopolymers or copolymers [9–13]. In the same line, extension of the rigid part by

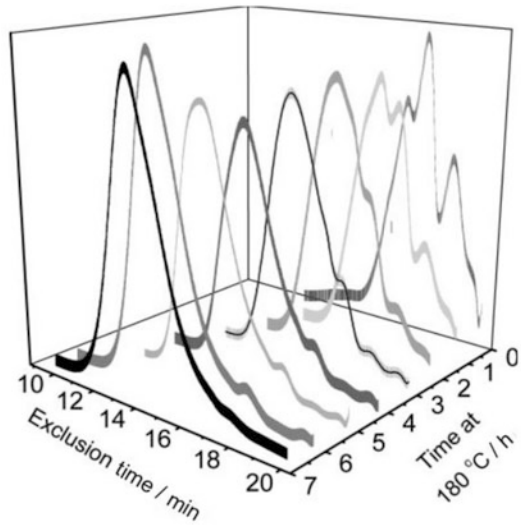

Fig. 5.2 Kinetic study of **Homopolymer's I** polymerization reaction via gel permeation chromatography (GPC). Reproduced from [9] with permission of Wiley-VCH Verlag GmbH & Co. KGaA

introducing two pyridine units per repeating unit combined with the introduction of aliphatic side substituents to improve solubility was also tested, see **Homopolymer III** [9].

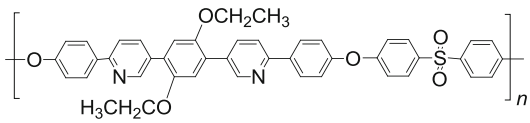

Homopolymer III

As was expected the homopolymer composed from the 2,5-bis(4-hydroxyphenyl) pyridine and bisphenylsulfone (**Homopolymer IV**) was completely insoluble in all practical solvents.

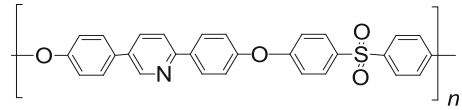

Homopolymer IV

A homopolymer with high basic unit content was desirable in order to create as many interaction sites with the phosphoric acid as possible, which led us to the design of the above-described homopolymers. However the encountered problems of solubility and plasticization softening of the doped membranes forced us to seek alternative structures and thus we designed copolymers that incorporated additional hydrophobic units in order to increase solubility. For that reason, a number of comonomers like the tetramethyl bisphenol [10] and the bisphenol A [13] were explored. These copolymers bearing pyridine units combined with diols having methyl substituents, like tetramethyl bisphenol (**Copolymer I**) and bisphenol A (**Copolymer II**), became a real breakthrough. From the numerous different copolymers synthesized and examined, those that combine the 2,5-bis (4-hydroxyphenyl) pyridine and the 3,3′,5,5′-tetramethyl-[1,1′-biphenyl]-4,4′-diol (**Copolymer I**) were easily soluble, even for higher pyridine diol contents, while at the same time preserving their mechanical properties and thermal and oxidative stability.

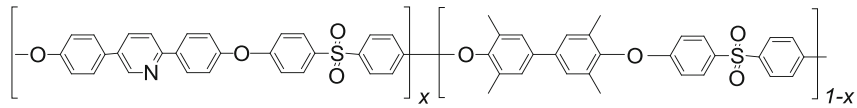

Copolymer I

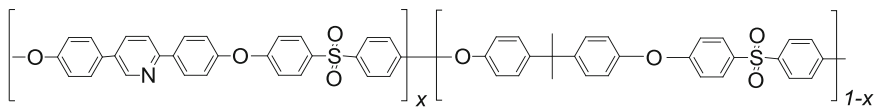

Copolymer II

In particular, for the **Copolymer I** with 60 mol% of the 2,5-biphenyl-pyridine diol in the main chain average molecular weights (MW)s up to 70,000 were obtained, while when 70 mol% of the same diol was employed MWs above 60,000 were achieved [10].

Almost all synthesized copolymers were soluble in common organic solvents regardless of their MW and showed excellent film-forming properties and high glass transition temperatures (T_g) up to 290 °C. Especially these high T_g values in all cases fulfill a major prerequisite for high-temperature PEMFC applications. Among the different compositions examined, the copolymer with 60 mol% pyridine units was selected as key copolymer for optimization of its preparation conditions that finally resulted in even higher molecular weights. This easily processable copolymer exhibits excellent film-forming properties, high glass transition temperature up to 280 °C, thermal stability up to 400 °C, and high oxidative stability.

The question of how critical is the oxidative stability of the materials used as membranes in fuel cells has been contradictory for long time. As it is known, PBI and PBI-related materials show a moderate stability in Fenton test conditions [14] while especially the doped PBI membranes lose their integrity within the Fenton test solution even after a few hours [15].

Fenton's test is a frequently used accelerated test for the oxidative stability of polymeric membranes [14]. According to this test, the membranes are exposed to a strong oxidative environment. More specifically, polymeric films are treated with 3 wt% H_2O_2 in the presence of ferrous ions at 80 °C for 72 h. Hydroxyl and hydroperoxyl radicals are created which lead either to chain scission or to ring opening of the benzene rings. In respect to the oxidative stability of the herein studied linear aromatic polyethers, all polymers were treated according to the Fenton's test conditions and remain intact after the treatment. This is proved by comparing the mechanical and thermal properties of the membranes before and after the treatment [16]. Also, blends of PBI with these aromatic polyethers resist Fenton's test [13], while PBI and its blends with sulfonated aromatic polysulfones did not withstand such a treatment [17]. The resistance to Fenton's test treatment could be due to the hydrophobicity of these aromatic polyethers, thus preventing the penetration of hydroxyl radicals, which can oxidize and disintegrate the polymeric membranes. To exclude this possibility hydrophilic blends of the linear **Copolymer I** [16] with a water-soluble polymer were tested. Depending on the blend composition, the water-soluble polymer was removed during the treatment of these blends with the Fenton's reagent and still the polymeric films maintained their mechanical integrity. The molecular characteristics of the polymers before and after the Fenton's test were determined by means of gel permeation chromatography (GPC) where the molecular weight distribution remained unchanged, thus proving the chemical stability of the polymeric films. Additionally, the spectroscopic characteristics of the treated polymers by means of Fourier transform infrared (FTIR) and nuclear magnetic resonance (NMR) were unaltered. Due to their high pyridine content, these copolymers can be doped with strong acids like the phosphoric acid, at doping levels up to 300 wt% depending on the copolymers' composition. Since conductivity is strongly dependent on doping level and temperature, for these copolymers conductivity values in the range of 10^{-2} S cm^{-1} were obtained at temperatures higher than 130 °C.

As mentioned before, another approach to improve solubility is the use of different non-substituted monomers that are randomly co-polymerized. Thus, non-substituted aromatic copolyethers containing main chain pyridine units were also synthesized by copolymerization of aromatic diphenols [11] and more particularly 2,5-bis(4-hydroxyphenyl) pyridine and 4,4′-biphenol or hydroquinone, **Copolymer III** and **IV**, respectively. Using the previously

developed methodology it was possible to synthesize such fully aromatic polyethers with high molecular weights, in some cases exceeding 100,000 (Mn value), but still keeping their solubility. Flexible and high quality membrane films were prepared that presented high glass transition temperatures (T_gs) and high decomposition temperatures (T_ds). The oxidative stability of the membranes was examined with Fenton's test and also in this case the membranes remained intact after the treatment. The doping ability and the proton conductivity of the membranes were also studied and the unsubstituted fully aromatic copolymers were indeed found potential polymeric electrolyte candidates for proton exchange membrane fuel cells. It should be emphasized that for this class of unsubstituted copolyethers the high doping values reached were realized without disturbing the para-aromatic character of the main polymeric backbones. By using the copolymerization approach we incorporated diols of different rigidity in order to disturb the structure regularity and subsequently the extent of the intermolecular interactions that are mainly responsible for insolubility problems [11].

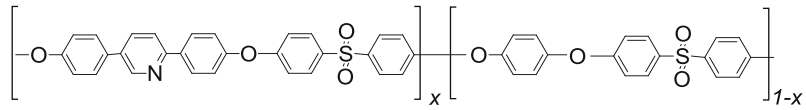

Copolymer III

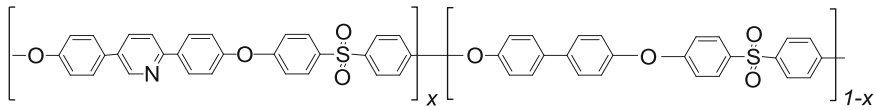

Copolymer IV

Overall, by using different approaches for the combination of the desirable properties a new family of linear aromatic polyethers able to be used as membranes for HT PEMFCs was successfully developed.

5.3 Side Group Functionalized Linear Aromatic Polyethers Containing Main Chain Pyridine Units

Side functionalities were used both as solubilizing groups and to impart specific functions based on the same polymeric backbone that was examined previously. As a first example on this category, side pyridine units were used in homopolymers and copolymers [18]. However limitations in molecular weight were encountered especially in the case of homopolymers and thus copolymers with the 2,5-bis(4-hydroxyphenyl) pyridine diol and the 1,4-dihydroxyl-2,5-di(3-or 4-pyridine)benzene diols were synthesized (**Copolymers V–IX**). The doping ability of these copolymers was greatly enhanced as the side pyridine diol content increased, reaching very high phosphoric acid uptakes but at the same time plasticization of the doped membranes was observed making their use in membrane electrode assemblies (MEAs) preparation and testing impossible [18].

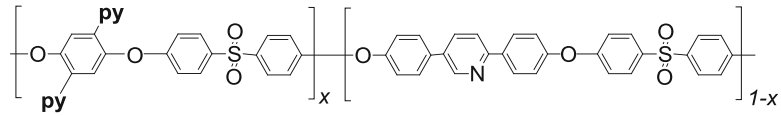

py : or

Copolymer V or VI

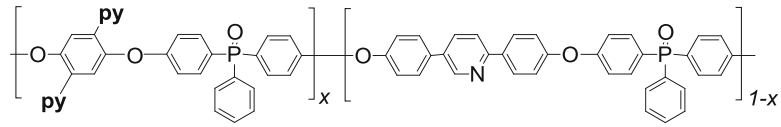

py : or

Copolymer VII or VIII

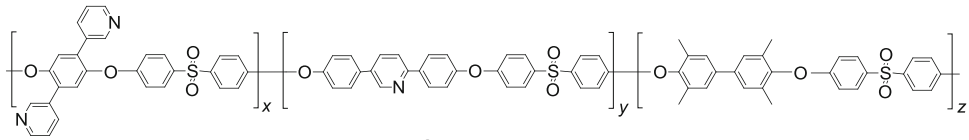

Copolymer IX

Taking into consideration all the positive and negative effects of the introduction of side pyridine units, a new generation of membranes was designed and synthesized incorporating the following monomers, the 2,5-bis(4-hydroxyphenyl) pyridine, a side pyridine diol, and as a third comonomer the tetramethylene bisphenol at selected and optimized ratios that provided the hydrophobic character which was necessary for the stabilization of the highly doped membranes (**Copolymer IX**) [19]. The success of this approach initiated a systematic exploration of the effect of the different functional groups on the membrane properties in terms of phosphoric acid doping ability and their influence on conductivity, doped membrane stability, and possible further reactivity.

In a subsequent approach bulky but not interacting with the H_3PO_4 substituents were chosen for the preparation of polymer electrolytes keeping the well-established pyridine-based aromatic polyether sulfone backbone [20]. In particular, phenyl and tolyl side moieties were introduced, **Copolymer X** and **XI**, respectively, since their size is expected to increase the free volume among neighboring polymeric chains in the bulk leading to an enhancement of the copolymers' doping ability without the plasticization phenomena of the previously pyridine-substituted copolymers.

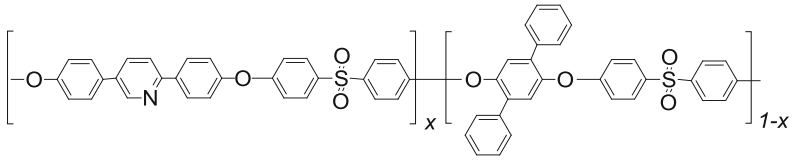

Copolymer X

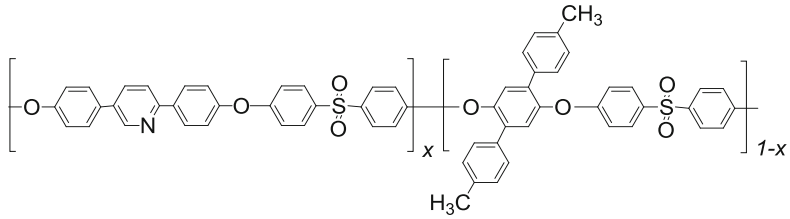

Copolymer XI

Both **Copolymers X** and **XI** were soluble in common organic solvents and as a result, they were characterized by means of ^{1}H NMR and via GPC. Excellent film-forming properties were observed only for the tolyl functionalized copolymers owing to their high MWs rising up to 45,000 (Mn). Membranes of ~100 μm having different pyridine content were examined for their doping in H_3PO_4 85 %. The acquired doping level (DL) increased with the polar pyridine content. This fact points out that with the side tolyl groups it was possible to obtain fully soluble and processable polyether materials of very high pyridine content and thus increased DL levels without plasticization of the doped membranes. The mechanical properties, T_gs up to 240 °C, and thermal stability, T_ds up to 450 °C, of these materials were not altered before and after Fenton's test.

Perhaps an even more interesting class of copolymers studied was that with carboxyl bearing moieties, **Copolymer XII** that was synthesized using an unprotected carboxylic acid containing monomer. High molecular weight copolymers with carboxyl group content up to 50 mol% were synthesized and characterized [20].

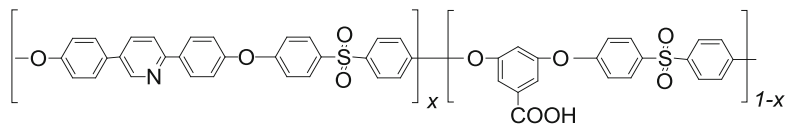

Copolymer XII

High DLs up to 450 wt% were obtained depending on the pyridine content of the polymers. Moreover, the presence of the carboxylic acid side groups did not decrease the doping ability of these copolymers. On the contrary the presence of the carboxylic acid functionalities led to higher DLs compared to the benchmark **Copolymer I**. High T_g and storage modules E' values were obtained for most of the **Copolymers XII** but most importantly exposure for as long as 3 weeks in Fenton's test oxidizing environment did not deteriorate the membranes even though the carboxylic acid side groups forced the solubility of these copolymers towards more polar solvents like dimethylsulfoxide.

Although these carboxylic acid copolymers are potential candidates for HT-PEMFCs, their most prominent feature was their use for further chemical cross-linking of the carboxylic acid side groups using different cross-linkers creating

stable 1,3,4-oxadiazole linkages as will be described later.

Phosphonate ester or phosphonic acid substituents have been additionally evaluated in an attempt to increase the interacting sites with the phosphoric acid doping agent along the polyelectrolyte macromolecular chains. These were strategically located as side groups in a diol monomer which was prepared by a phosphorus-carbon coupling reaction of tetrahydropyranyloxy diprotected 2,5-dibromo-1,4-dihydroxy benzene with diethylphosphite. Either in the phosphonate ester or in the phosphonic acid form the diol was used in polymerizations with the bis (4-fluorophenyl) sulfone or bis(4-fluorophenyl) phenylphosphinoxide as well as with the 2,5-diphenyl-pyridine diol and the tetramethyl-biphenyl diol in copolymers and terpolymers, respectively [21]. However, these synthetic efforts resulted in homo and copolymers of high thermal stability but moderate molecular weights. Only the terpolymers (**Copolymer XIII**) could be obtained in higher molecular weights. These phosphonated polyethers were used also for the preparation of blends with the extensively studied **Copolymer I**. For the copolymers and terpolymers it was shown that the combination of the phosphonic acidic groups with the basic pyridine comonomers resulted in polymers with increased thermal stability. Furthermore, it was shown that the incorporation of high percentages of phosphonic acid groups reduces the doping ability of the final blend due to possible interactions of the acidic units with the pyridines.

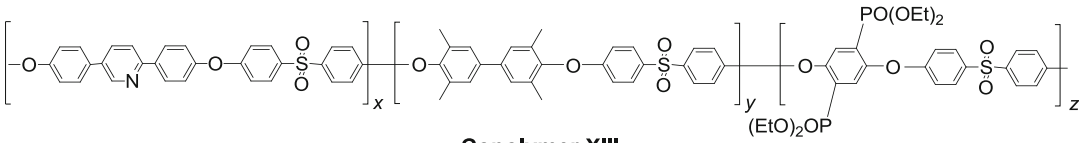

Copolymer XIII

A series of aromatic polyethersulfones bearing pyridine main chain groups and side sulfonic acid groups were reported (**Copolymer XIV**) [22]. The driving force was to combine the thermal and chemically stable macromolecular backbones with the phosphoric acid interacting pyridines and the water interacting sulfonic acid moieties.

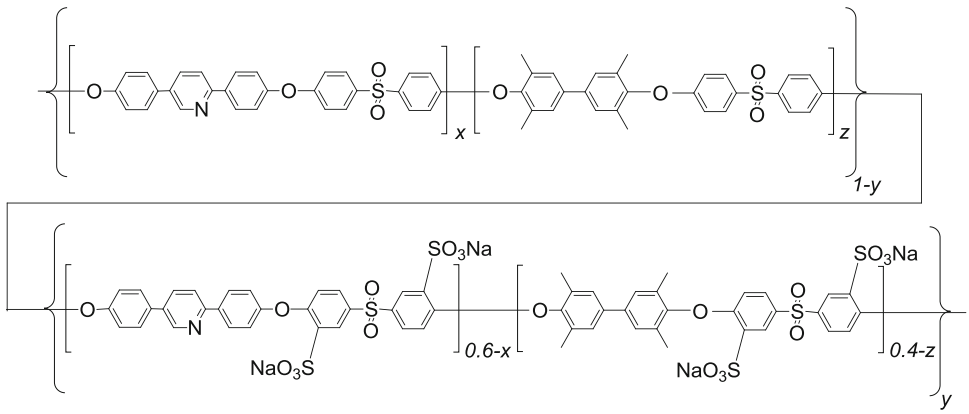

Copolymer XIV

All copolymers with sulfonation degree (SD) = 0–80 % showed excellent film-forming properties and the dynamic mechanical analysis (DMA) gave T_g values that increased with the sulfonation degree, up to 350 °C in the sodium salt form, which increased even further reaching

370 °C in the acidic form. The oxidative stability of the copolymers was higher than relevant aromatic sulfones like sulfonated poly(arylene ether sulfone). The water uptake of the sulfonated copolymers was about 30 wt% at 80 °C. On the other hand, the introduction of sulfonate groups onto the main chain decreased the ability of absorbing phosphoric acid due to interactions of the acidic groups with the basic pyridine moieties.

In an additional effort side hydroxyl groups have been incorporated onto the well-established aromatic polyether sulfone backbones bearing the polar pyridine units in the main chain (**Copolymers XV** and **XVI**). The side chain hydroxyl moieties were further transformed to propargyl moieties. Both cases aimed mainly at preparing chemically cross-linkable linear polymers either through thermal treatment or through etherification with polyfluorine bearing aromatic cross-linkers [23]. Initially dimethoxy diol monomers were designed, which after the high temperature polycondensation with the respective comonomers were deprotected to the hydroxy-based analogs by ether cleavage with boron tribromide.

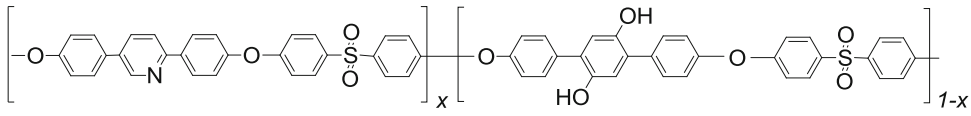

Copolymer XV

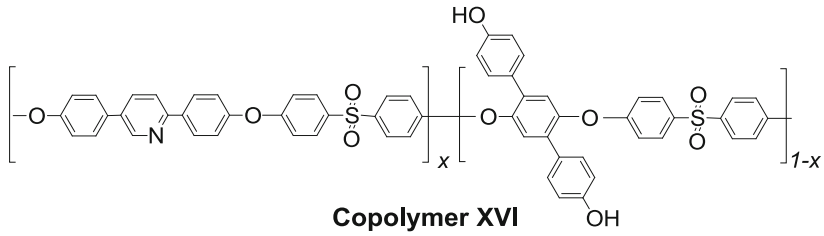

Copolymer XVI

In another attempt double bond side functionalities were introduced onto pyridine-based aromatic poly(ether sulfone)s. The ultimate scope of this approach was the cross-linking of the active double bonds after polymerization and after the preparation of the desired polyelectrolyte membranes in order to mechanically and thermally stabilize the doped membranes, as will be described below in greater detail.

The initial concerns for the viability of the double bonds during the high temperature condensation polymerization were overcame both for allyl (**Copolymers XVII–XX**) [24, 25] and styryl (**Copolymers XXI**) [26] side group containing copolymers. In all these cases special attention was paid to the optimization of the polymerization conditions in order to keep the double bonds intact. Combined FTIR and NMR characterizations were employed and the copolymers content in double bonds was checked after the different polymerization processes.

In particular, for the allyl containing monomer a high temperature isomerization-rearrangement of the allyl groups of 2,2′-diallyl bisphenol A into propenyl groups was observed during the polymerization reaction. Of course the propenyl moieties retain their reactivity as double bonds, which is the major requirement for their further cross-linking. The observed rearrangement was attributed to the fact that the potassium carbonate acts as a catalyst of isomerisation of allyl groups to propenyl groups. As shown in the below NMR spectra (Fig. 5.3), the double bond protons of the propenyl groups appear at 6.2 and 6.5 ppm. The percentage of the double bonds in the polymeric chain was calculated from the integration ratio of the peak of the aromatic proton neighboring the nitrogen in the pyridine ring and the peaks of the propenyl groups.

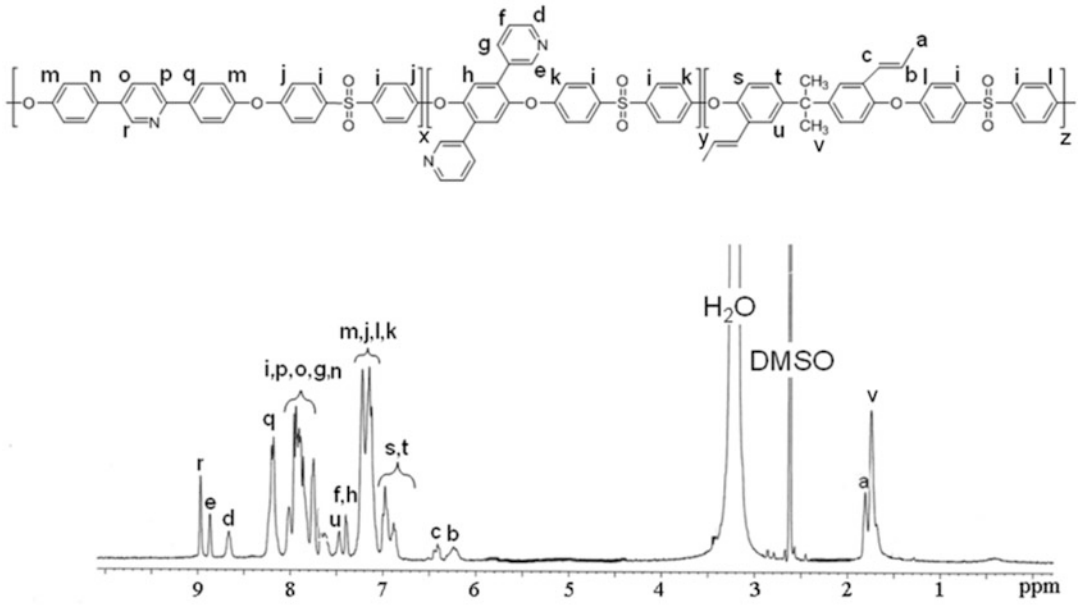

Fig. 5.3 [1]H NMR spectrum of the propenyl functionalized cross-linkable **Copolymer XX**. Reproduced from [25] with permission of Elsevier

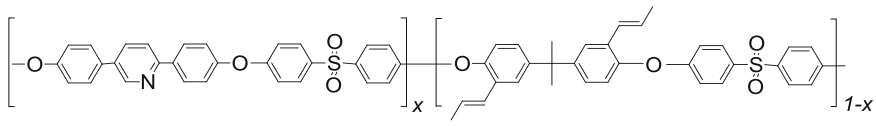

Copolymer XVII

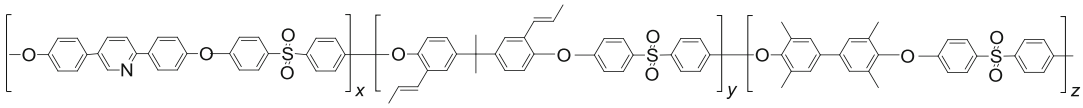

Copolymer XVIII

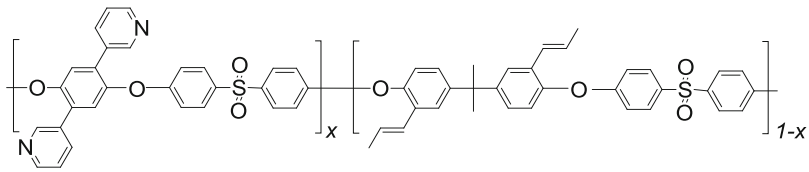

Copolymer XIX

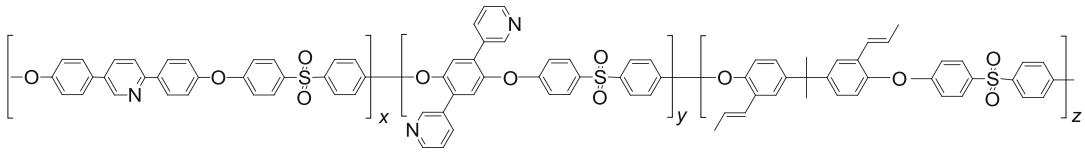

Copolymer XX

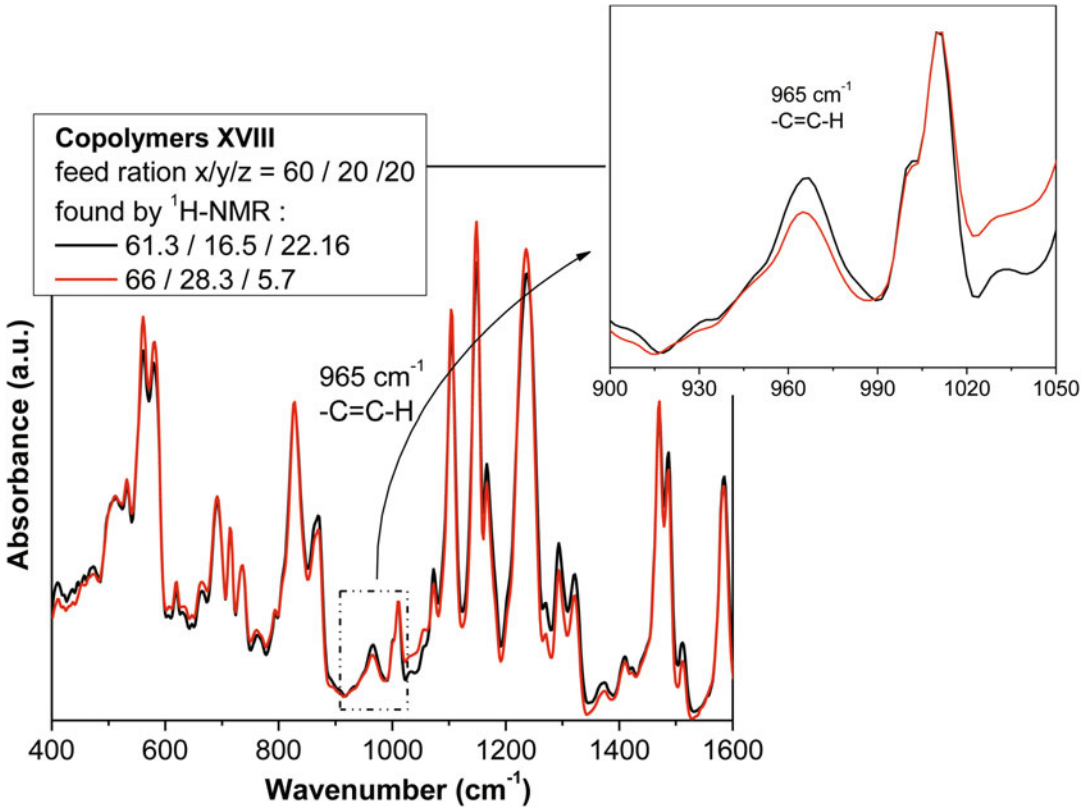

Fig. 5.4 ATIR spectra of **Copolymers XVIII** with identical initial monomers' feed ratio ($x/y/z = 60/20/20$) but with different polymerization reaction conditions resulting in different calculated ratios of the final materials, *Inset*: enlargement of the area 900–1050 cm^{-1}

As already mentioned great care was devoted to the optimization of the polymerization conditions not only in terms of maintaining the side double bonds after the course of the reaction but also in achieving the desired double bond content. A representative example is shown below where **Copolymers XVIII** with the same monomers feed ratio show different double bond content depending on the preparation conditions. Besides the ^{1}H NMR characterization of such double bond functionalized materials their FTIR characterization was proven even more valuable for the calculation of the double bond percentage in the final polymeric materials (Fig. 5.4) based on the characteristic and well-resolved peak at 965 cm^{-1}. Since all the resulting polymers were soluble in polar organic solvents, their characterization using GPC took place proving their high molecular weights in all cases.

Fenton test treatment was also performed in these materials in order to evaluate whether the membranes are able to withstand a strong oxidizing environment during the fuel cell operation. The oxidative stability of these copolymers after treatment with the Fenton reagent was examined with dynamic mechanical analysis and thermogravimetric analysis where no significant changes occurred after treatment with hydrogen peroxide neither to the membrane's integrity nor to its mechanical properties

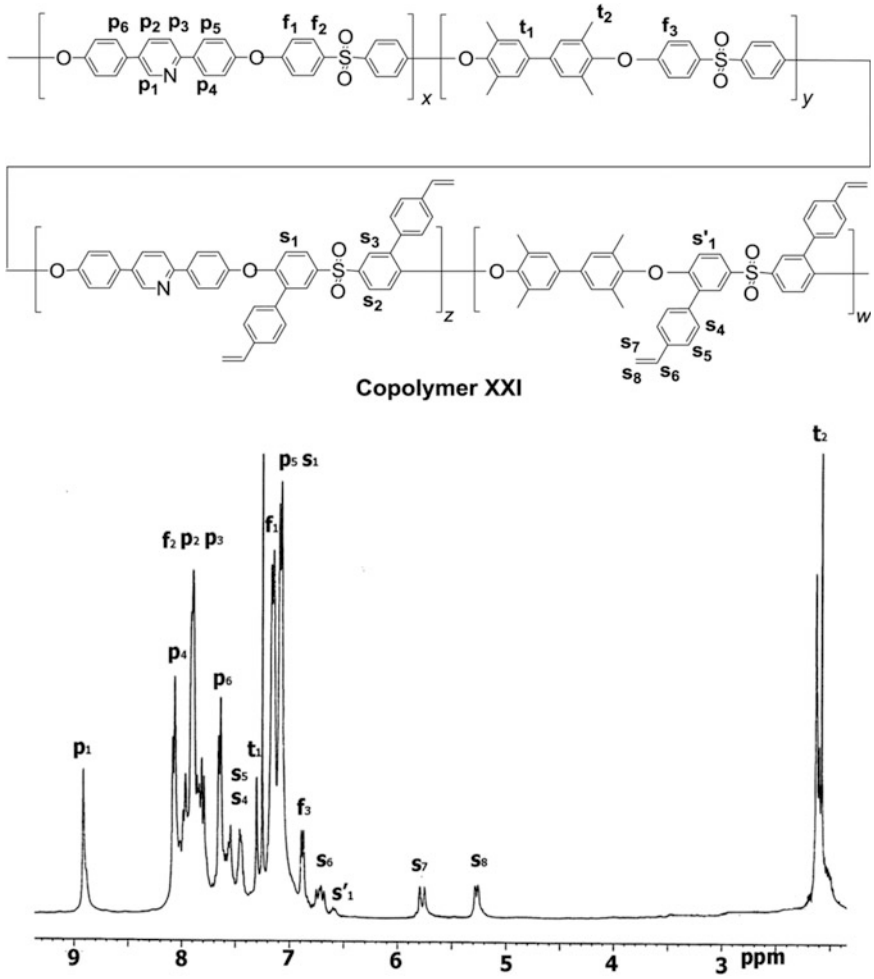

Fig. 5.5 **Copolymers XXI** with cross-linkable side styrene functionalities and an ^{1}H NMR spectrum the copolymer with $x + z = 80$, $z + w = 20$, in $CDCl_3$ with peak assignment. Reproduced from [26] with permission of Elsevier

compared to the polymer before such a treatment. Moreover, the thermal stability of the treated membrane shows a further improvement, probably due to the cross-linking reactions that can happen during the Fenton test treatment.

For the styrene side functionalized **Copolymers XXI** the general structure of the resulted copolymers is given in Fig. 5.5 together with a representative ^{1}H NMR spectrum at which the protons of the "living" side double bond are observed at 5.3, 5.8, and 6.7 ppm [26]. Copolymers with several percentages of the pyridine diol as well as the difluoride monomer bearing the side double bond functionalities were obtained. These copolymers were easily soluble in common organic solvents in all compositions synthesized and thus besides their characterization by means of ^{1}H NMR for the confirmation of the proposed structure and the copolymer composition, their molecular characteristics were evaluated by GPC giving molecular weights between 10,000 and 20,000. The mol percentage of the vinylbenzene groups was close to the theoretically expected as calculated from the ^{1}H NMR spectra using the integration of the peaks attributed to the protons of the vinyl groups and of the peak of the proton

next to the nitrogen in the pyridine unit. As proven by ^{1}H NMR, the double bonds remain intact under the polymerization conditions and can be used for further reaction as will be explained in the below section.

5.4 Cross-Linked Aromatic Polyethers Bearing Pyridine Main Chain Units

A crucial problem of all the polymer electrolytes is the deficient long-term durability of these systems at temperatures as high as 200 °C. The challenge to find materials that show even greater mechanical stability with adequate ionic conductivities was the driving force for extensive research efforts. An effective approach to overcome this problem is the covalent cross-linking. Via the cross-linking route a large, stable network of anchored polymeric chains is achieved, which stabilizes the membrane and improves its mechanical properties. So the possibility to create cross-linked polymers able to be used as membranes at higher operating temperatures was explored by our group. In the course of these efforts to prepare chemically cross-linked high temperature polymer electrolytes, different chemistries having as baseline the chemical and thermal stability of the fragments have been explored. The different side functionalities used for cross-linking of the membranes were side double bonds and side carboxyl groups, as an attempt to create stable cross-linking bonds for even more robust and stable proton conducting polymeric electrolytes that can be used as the core parts of membrane electrode assemblies (MEAs) for HT-PEMFCs.

As a first approach, copolymers and terpolymers combining main chain pyridine units, cross-linkable carboxylic acid side groups, and/or hydrophobic methyl groups were cross-linked [27]. The carboxylic acid groups can lead to thermally and chemically stable bond formation, as, for example, the creation of imidazole or oxadiazole rings. Thus, in our approach we explored and optimized different methods for cross-linking the carboxyl bearing polymers creating oxadiazole cross-linking groups providing new membranes that were tested in single cells operating at temperatures higher than 200 °C. Initially, **Copolymers XII** of high molecular weights with side carboxylic acid groups, having good film-forming properties and mechanical integrity, were employed as precursors for cross-linking. The formation of 2,5-substituted-1,3,4-oxadiazole bridging linkages was chosen due to their high thermal and chemical stability. Two different routes were used for the covalent cross-linking (Scheme 5.2), the phosphorylation or Higashi process [28, 29] where terephthalic dihydrazide (TDH) was the cross-linking agent and the Huisgen procedure [30, 31] where carboxylic acid chlorides reacted with phenyl bis-tetrazole (BTT). In both methods, the amount of the cross-linking agent was stoichiometric and calculated based on all active carboxylic sites along the polymeric chain.

In the first case, a two-step procedure was followed in order to obtain the final cross-linked oxadiazole containing membranes, where the second step was the cyclodehydration of the intermediate to the final 1,3,4-oxadiazole bridged polymer that was accomplished by heating the membrane under vacuum for several hours at temperatures from 160 °C and up to 320 °C. In the second case, according to the Huisgen method the oxadiazole group was synthesized through the initial nucleophilic substitution of an acylating agent to the nitrogen of the tetrazole moiety. The acylating agent attacks the tetrazole ring resulting in a ring opening at 2,3-position and a recyclization process is followed through the acyl oxygen with simultaneous loss of a neutral nitrogen molecule. A similar procedure was followed in this work for cross-linking the carboxylic acid bearing polymers. Specifically, carboxylic acid groups of the polymeric chains were modified through $SOCl_2$ to carboxylic acid chlorides. The latter played the role of the acylating agent of the BTT cross-linker, forming the final oxadiazole cross-linked polymer. The

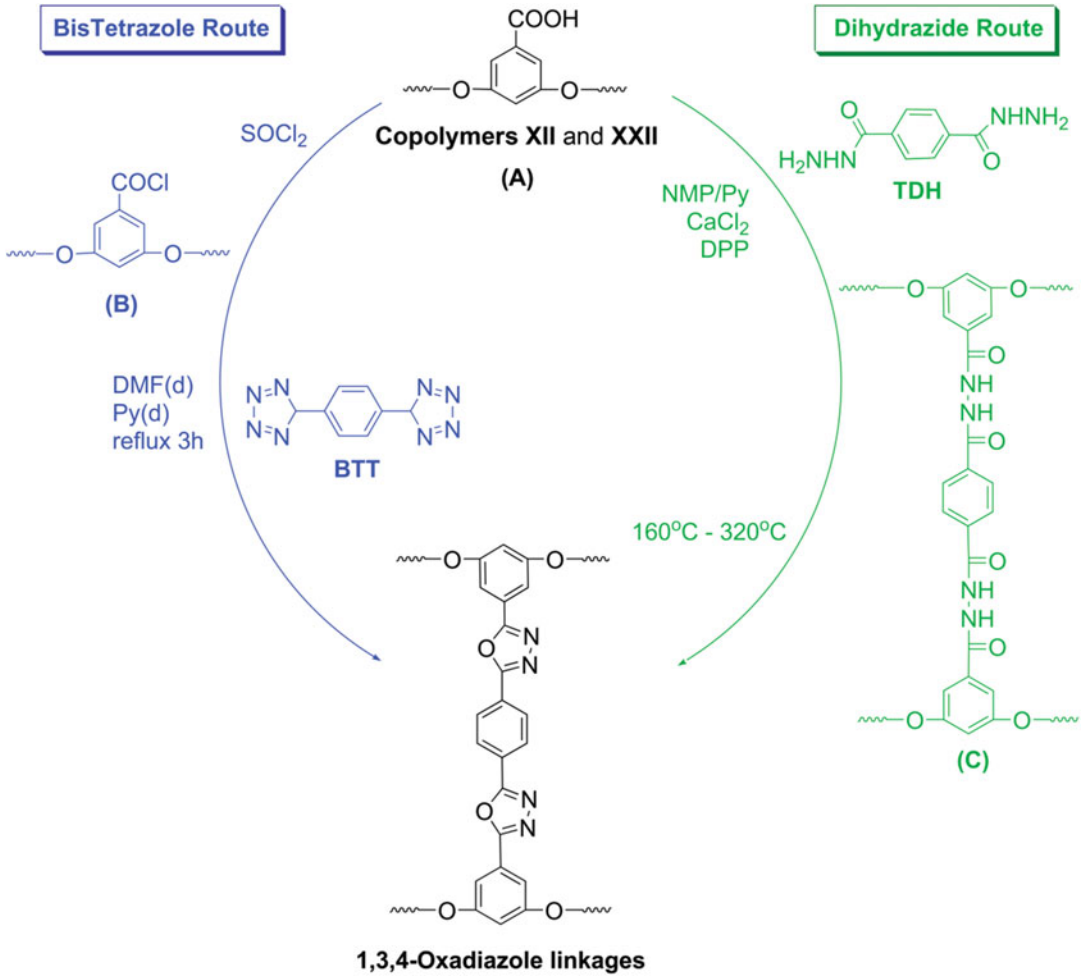

Scheme 5.2 Cross-linking methodologies applied to carboxylic acid bearing aromatic polyethersulfones (**Copolymers XII** and **XXII**) using terephthalic dihydrazide (TDH) or bistetrazole (BTT) as the cross-linking agents. Reproduced from [27] with permission of the Royal Society of Chemistry

two methods are schematically shown in Scheme 5.2 and both methodologies were optimized using as criterion the cross-linked membrane's solubility in organic solvents and also the cross-linked membrane's quality and integrity.

Using the optimized conditions cross-linked membranes with significantly increased glass transition temperatures T_g were obtained for both methodologies as shown in Fig. 5.6. Differences between the two cross-linking methodologies can be observed from the DMA results of the membranes before and after cross-linking. As can be seen in Fig. 5.6, the cross-linked membrane through the dihydrazide route (**Copolymer $\mathbf{XII_{CL\text{-}TDH}}$**) has a glass transition temperature increased by 25 °C compared to that of the initial copolymer, whereas the cross-linked membrane through the bistetrazole route (**Copolymer $\mathbf{XII_{CL\text{-}BTT}}$**) showed an even higher increase of 75 °C. Based on these results and also on a detailed analysis of the thermal stability and solubility of the cross-linked copolymeric membranes, the superiority of the cross-linking methodology through the bistetrazole (BTT) route was proved. Thus, this particular route

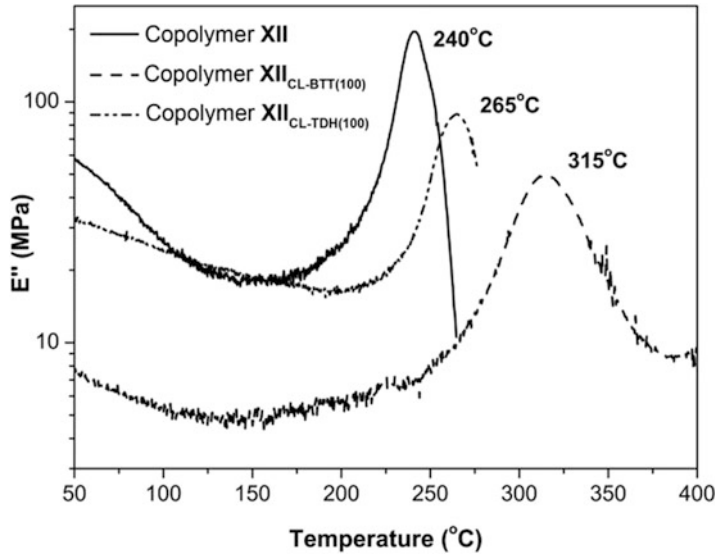

Fig. 5.6 Comparison of the temperature dependence of the loss (E'') modulus for the linear **Copolymer XII** and of the cross-linked copolymers **Copolymer XII$_{CL-TDH(100)}$** and **Copolymer XII$_{CL-BTT(100)}$**. Reproduced from [27] with permission of the Royal Society of Chemistry

was chosen and further optimized for the cross-linking of the respective terpolymers that additionally incorporated the tetramethyl-biphenyl diol (**Copolymer XXII**).

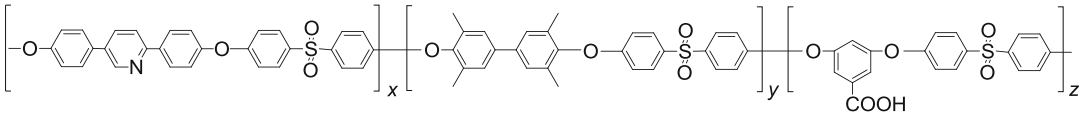

Copolymer XXII

The doping ability of the cross-linked membranes was also evaluated. Figure 5.7 presents an example of the cross-linked terpolymer through the bistetrazole route (**Copolymer XXII$_{CL=BTT}$**) with 100 % cross-linking degree impregnated in H_3PO_4 85 % at 80 °C and at 100 °C compared to the linear precursor **Copolymer XXII**. In general the cross-linking leads to a more compact chemical structure and as a result the doping ability of cross-linked membranes is expected to decrease. However, there have been some distinct cases at which the doping ability of the cross-linked materials was superior to the initial membranes usually attributed to the introduced functionalities which also interact with the phosphoric acid. Also in herein cross-linking through oxadiazole formation case, the doping ability of the cross-linked polymers was enhanced compared to their linear analogues since the formed oxadiazole rings can also interact with phosphoric acid contributing, thus, to the overall acid uptake of the final cross-linked membrane [32]. This fact strongly denotes the role of the chemical structure and the resulting morphology on the materials' properties.

The second general approach for the covalent cross-linking was the use of side double bond functionalized copolymers [24]. In this case the synthesis of aromatic polyethers containing polar pyridine units in the main chain and side cross-linkable propenyl groups was the key step. These polymers were subjected to thermal cross-linking with the use of a cross-linker. The effect of the cross-linking on the thermal and mechanical

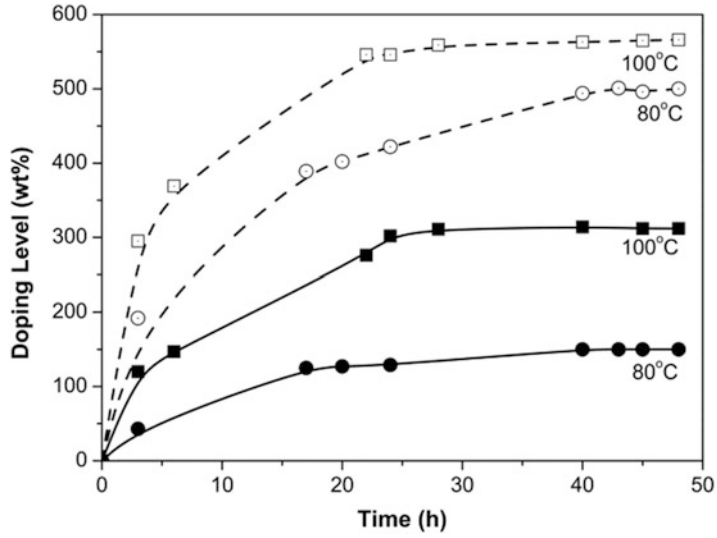

Fig. 5.7 Time dependence of the doping level of the linear **Copolymer XXII** (*filled symbols*) and its 100 % cross-linked counterpart **Copolymer XXII$_{CL=BTT}$** (*open symbols*) at 100 °C and 80 °C, respectively. Reproduced from [27] with permission of the Royal Society of Chemistry

properties and on the phosphoric acid doping ability of the membranes was studied.

In particular, a detailed study of the cross-linking procedure was performed in order to optimize the cross-linking conditions. During the thermal treatment the bisazide used as cross-linker looses one nitrogen and thus a reactive nitrene is formed. This intermediate product is added to the propenyl groups producing aziridines and amines. The cross-linked structure was confirmed by comparing the FTIR spectra of the pristine and the cross-linked polymers and a characteristic example is given in Fig. 5.8 for the **Copolymer XVII**. The absorption peak at 965 cm^{-1} assigned to the C=C double bonds decreased after the cross-linking procedure while a new broad band at 3374 cm^{-1} appeared in the cross-linked polymer which is attributed to the N–H stretch vibration of the secondary amines. All the membranes which were successfully cross-linked were almost insoluble in all organic solvents.

The effect of the cross-linking on the mechanical properties of the membranes was examined with DMA measurements. The glass transition temperatures of the cross-linked membranes were increased compared to the virgin polymers, as shown, for example, in Fig. 5.9 where the cross-linked membrane has a T_g value at 290 °C which is 62 °C higher compared to the not cross-linked membrane. Furthermore, the storage modulus after cross-linking is not decreased after 300 °C but it reaches a plateau and this behavior is characteristic of cross-linked networks. The cross-linked membranes were subjected to treatment with the Fenton's reagent in order to evaluate their oxidative stability. In all cases they preserved their mechanical properties showing thus the high oxidative stability of the cross-linked structures.

The doping ability of the cross-linked membranes in phosphoric acid at 80 °C in comparison with the doping level of the virgin polymers revealed that these cross-linked membranes showed higher doping levels compared to the neat polymers. That was attributed to the fact that the formation of the aziridines or amines functionalities could also interact with the phosphoric acid resulting in higher doping levels.

The exact chemical structure of the side double bonds is a crucial parameter in respect to their stability but also their reactivity. Thus, the allyl groups used above were thermally transformed to propenyl side group but the latter present lower reactivity to thermal polymerization due to sterical reasons.

An alternative approach was the case of **Copolymers XXI** bearing styrenic side functionalities [26] that would enable the

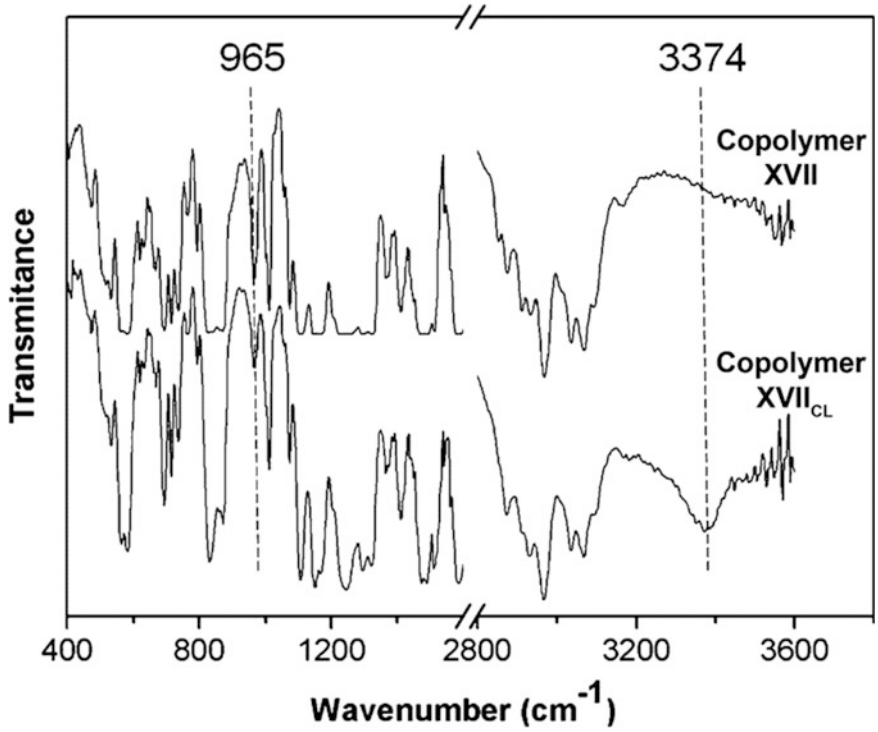

Fig. 5.8 Comparative FT-IR spectra of the pristine linear **Copolymer XVII** and its cross-linked analogue **Copolymer XVII$_{CL}$**. Reproduced from [24] with permission of the American Chemical Society

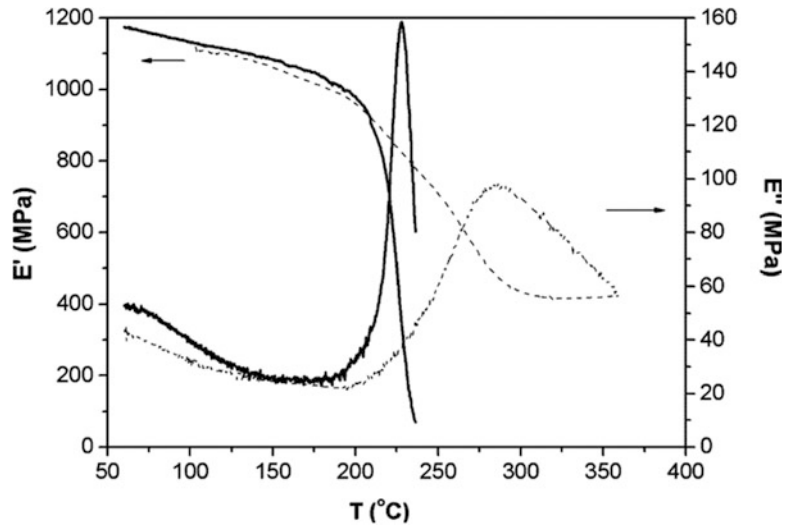

Fig. 5.9 Comparative DMA curves of the virgin **Copolymer XVII** (*solid line*) and the cross-linked polymer **Copolymer XVII$_{CL}$** (*dashed line*). Reproduced from [24] with permission of the American Chemical Society

covalent cross-linking by thermal treatment. In this case, the active vinyl bonds were chosen over propenyl moieties as more drastic to cross-linking by thermal treatment without the need of a cross-linking agent. **Copolymers XXI** were subjected to post-polymerization cross-linking by thermal treatment of the membranes at 250 °C under inert atmosphere for 12 h towards

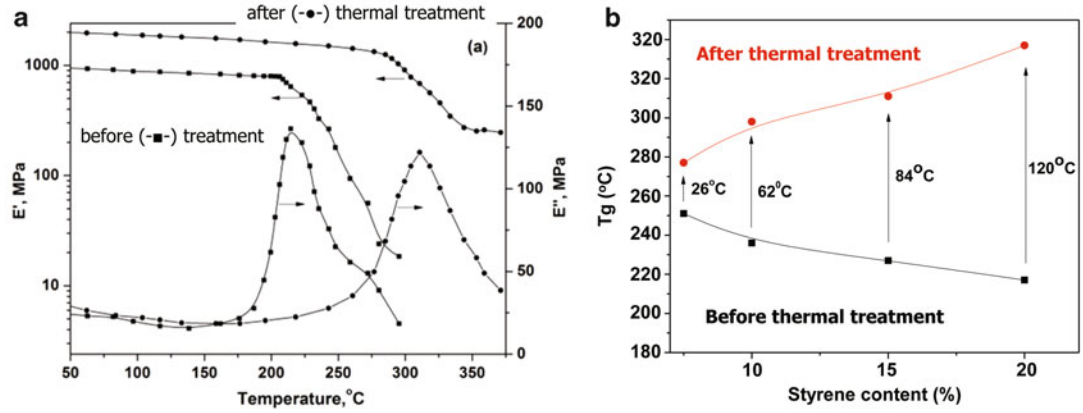

Fig. 5.10 (**a**) DMA diagrams of **Copolymer XXI** with $x + z = 60$ and $z + w = 15$ before (*filled square*) and after (*filled circle*) thermal treatment; (**b**) comparison of the T_g values of the linear **Copolymers XXI** (*black line*) and of their cross-linked counter parts after thermal treatment **Copolymers XXI$_{CL}$** (*red line*)

the formation of a stable network. The initial **Copolymers XXI** showed T_g between 200 and 250 °C, thus the temperature of 250 °C was selected for the thermal treatment since thermal cross-linking is enhanced at temperatures above the T_g [33, 34]. All initial linear copolymers depicted good solubility in organic solvents, whereas the thermally treated membranes were almost insoluble under the same conditions indicating their successful cross-linking. The effect of the cross-linking on the mechanical properties of the membranes was examined by DMA measurements. As it is shown in Fig. 5.10, the glass transition temperatures of the linear precursors were drastically increased after their thermal treatment. More specifically, increase of the vinyl bond content in the initial copolymer and consequently increase of the cross-linking density after thermal treatment resulted in higher change of the T_g, ΔT_g, leading to superior T_g of the cross-linked polymers reaching values well above 300 °C enabling their use as high temperature polymer electrolytes.

During the above studies of the cross-linking of the side double bonds containing aromatic polyethers it was realized that the membranes' solubility in polar solvents was significantly reduced during the doping of the non-cross-linked linear membranes even those having large contents of side pyridine units. That observation was contradictory to our previous experience where membranes with high side pyridine contents were extensively plasticized by phosphoric acid which was accompanied by loss of their mechanical properties rendering them unsuitable for MEA preparation [18]. A careful consideration of these two cases helped us to address and achieve our ultimate target. That is the preparation of thermally stable polymer electrolytes, which will be able to retain higher amounts of strong acids without losing their mechanical integrity aiming at their application in fuel cell devices with operating temperatures up to 220 °C [25]. Thus, cross-linkable linear copolymers having side pyridine moieties and side double bonds attached to the polymeric backbone were cross-linked during doping in phosphoric acid (**Copolymers XIX** and **XX**). More specifically the cross-linking was processed by cationic polymerization during the doping procedure in which the phosphoric acid acts as cationic initiator for the opening of the double bonds at high doping temperatures ranging from 80 to 120 °C as it is schematically shown in Scheme 5.3. Strong protonic (Brønsted) acids can initiate cationic polymerizations [35]. The propagation proceeds via the addition of the double bonds to the cation and the cross-linked network is formed.

In order to confirm the successful cross-linking, samples of the membranes were immersed in acid for different times and

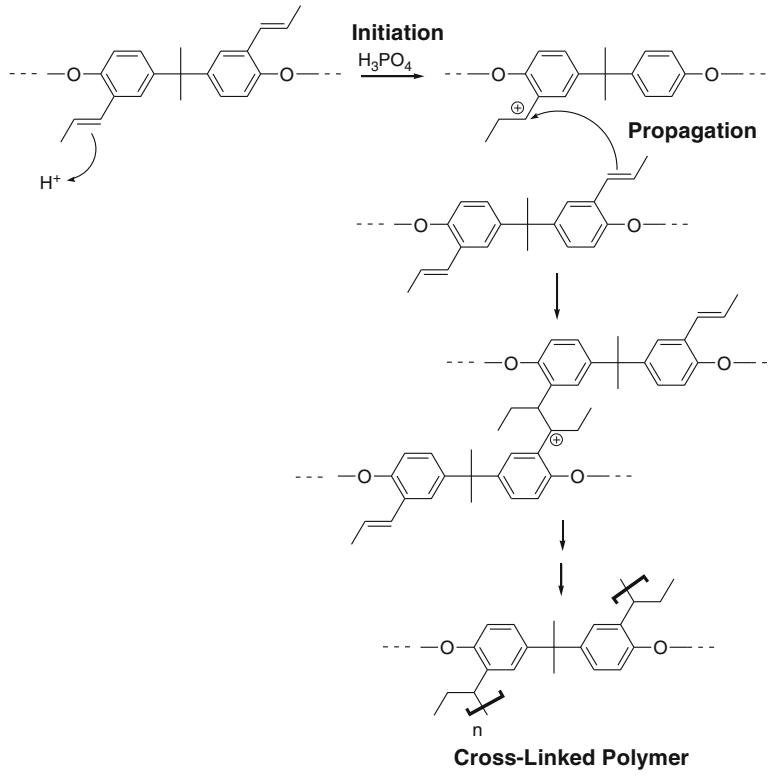

Scheme 5.3 Schematic representation of the cross-linking in phosphoric acid through cationic polymerization. Reproduced from [25] with permission of Elsevier

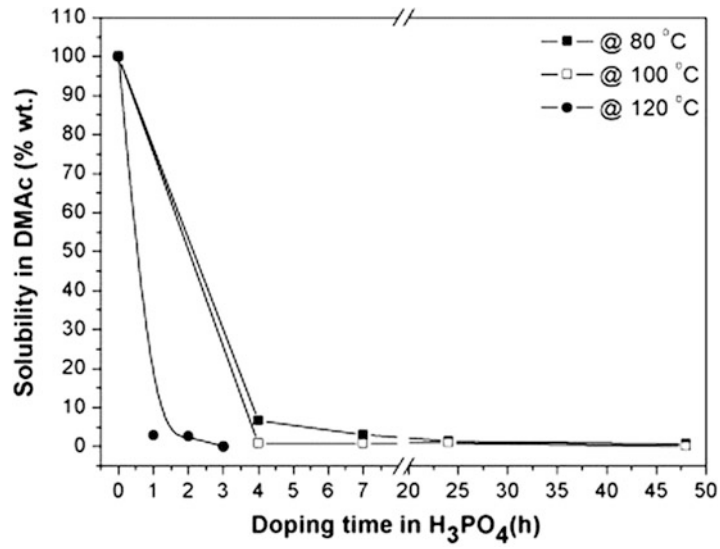

Fig. 5.11 Solubility dependence versus the doping time in phosphoric acid at different temperatures, for the cross-linked **Copolymer** $\mathbf{XX_{CL}}$. Reproduced from [25] with permission of Elsevier

temperatures and their solubility in *N*,*N*-dimethylacetamide (DMAc) was tested. Figure 5.11 depicts the solubility dependence versus the doping time in phosphoric acid at different temperatures for the cross-linked **Copolymer XX**. Initially the membranes are completely soluble in DMAc, while the solubility of the acid treated membranes is gradually

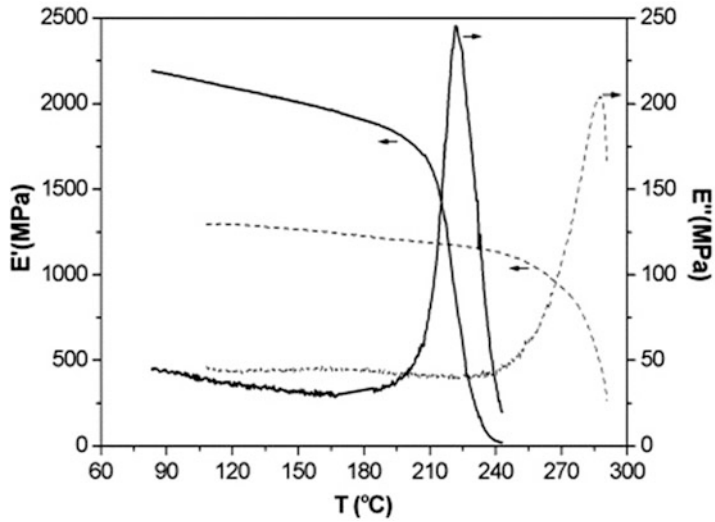

Fig. 5.12 Comparative DMA curves of the virgin **Copolymer XX** (*black line*) and the cross-linked in phosphoric acid **Copolymer XX_{CL}** (*dashed line*). Reproduced from [25] with permission of Elsevier

reduced as the doping time increases and only few hours are required to obtain almost insoluble materials. Additionally increase of the temperature reduces the time required for the formation of the cross-linked network. The cross-linking reaction was also followed spectroscopically using FTIR where the peak at 965 cm^{-1} which is assigned to the C=C double bonds (as shown in Fig. 5.8) clearly decreases in the case of the acid treated membrane.

The efficient cross-linking was also confirmed by the mechanical properties evaluation of the cross-linked membranes that presented a T_g value of 285 °C, which is about 65 °C higher compared to the initial terpolymer (Fig. 5.12). Additionally the decomposition temperature of the acid treated cross-linked membranes showed an increase by 125 °C reaching T_d values above 400 °C, while the pristine terpolymers were thermally stable up to about 280 °C.

All these results prove the successful cross-linking of the double bonds via cationic polymerization. This was the first report of such a cross-linking during the acid doping procedure of polymer electrolyte membranes. The breakthrough of this cross-linking methodology is in its simplicity since the membranes can be prepared by casting, evaluated thoroughly for their quality while still maintaining their solubility, and in a final step and at any desired time, they can be cross-linked during the doping procedure. Thus, during this new process it is possible to obtain a cross-linked network without adding further steps and additional costs to the overall production sequence. This is of high importance in view of the fact that for the commercialization of fuel cells an important parameter which has to be taken into consideration, along with the least possible cost, is the easiness and reproducibility of the electrolytes' preparation procedure.

5.5 Interaction of Phosphoric Acid and Water with the Polymer Membranes

As mentioned in the previous sections, the electrolyte materials are doped with H_3PO_4 in order to assure high proton conductivity. Acid uptake is a result of the interactions of the polar basic pyridine group with phosphoric acid. The pyridine ring can react and be protonated by H_3PO_4 [7, 36, 37] as illustrated in Fig. 5.13a. These specific interactions were surveyed and demonstrated by means of FT-Raman spectroscopy. Spectra of **Copolymer I**, pristine and after gradual doping with phosphoric acid are depicted

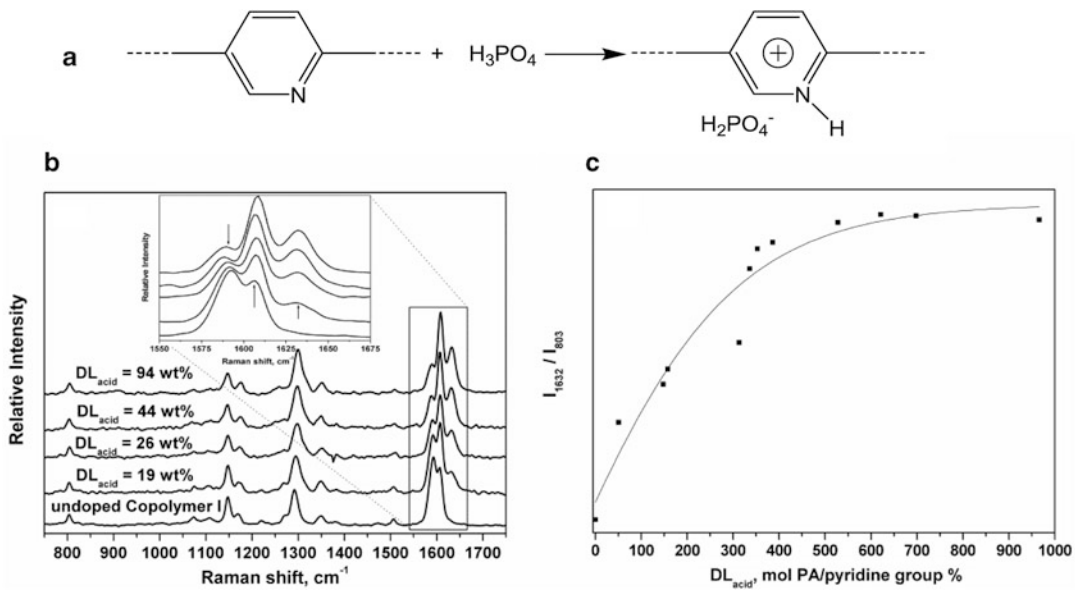

Fig. 5.13 (**a**) Interaction of phosphoric acid with the pyridine polar group of **Copolymer I**; (**b**) Raman spectra of **Copolymer I** before and after doping with H_3PO_4 85 wt% at several doping levels; (**c**) ratio of relative intensities versus acid doping level expressed in mol H_3PO_4 (PA) per polar group (%) for the peaks 1632 and 803 cm^{-1} for **Copolymer I**/H_3PO_4. Reproduced from [37] with permission of the Royal Society of Chemistry

in Fig. 5.13b. Upon doping, the pyridine groups are protonated, as shown by the blue shift from 1593 to 1608 cm^{-1} of the absorption peak of the pyridine group in the Raman spectrum and the appearance of a new peak at 1630 cm^{-1}. This characteristic shift is attributed to the positive charge that is being induced on the N atoms by the phosphoric acid. For the PBI-based materials, a corresponding shift takes place of the symmetric stretch of the imidazole group from 1539 to 1570 cm^{-1}. In the latter case, the Raman shift is larger denoting stronger interaction of the imidazole ring with the acid, which is justified by its stronger basic character compared to pyridine (60 times more basic, the pK_a of the conjugate acid is about 7, whereas for pyridine it is 5.2 [38]).

The difference in the specific interactions between the two groups is reflected on the doping procedure. The ratio of the peak at 1632 cm^{-1} that appears upon acid doping for **Copolymer I** to the unaffected peak at 803 cm^{-1} was calculated, Fig. 5.13c. The doping levels are expressed in moles of phosphoric acid per polar group. Complete protonation of all the pyridine units takes place when the ratio reaches its maximum constant value. As can be seen, three molecules of acid per repeat unit, or else five molecules of acid per polar group are needed in order to reach to the full protonation of the pyridine moieties. On the contrary, in the case of PBI each acid molecule entering the matrix protonates one imidazole group [37, 39].

These interactions though of ionic nature could not possibly contribute significantly to the ionic conductivity of the membrane due to the limited network of the H_3PO_4 molecules, as well as the size and the immobilization of the species involved. Thus the acid uptake leading to full protonation is not sufficient to lead to high proton conduction values. Instead they constitute the substrate on which the excess phosphoric acid network will be developed within the matrix. The high proton conductivity is facilitated by this excess amount of acid beyond the primary protonation, which through hydrogen bonding forms a continuous network for the proton conductivity. For a given structure, conductivity

increases with acid uptake since the unbound acid [40] is mainly responsible for the conductivity [39, 41].

The doping behavior of the different polymeric polyether type materials mentioned in the previous sections is reported after immersion in 85 wt% phosphoric acid at various doping temperatures. The acid uptake is not always proportional to the percentage of the polar group in the (co)polymer chain. In fact, it has been proven that the acid doping ability, as well as the ionic conductivity, is strongly influenced by the chemical structure [12, 20, 42]. The monomers used, their ratio, the presence of different side functionalities, and the density of the polar pyridine groups define the final acquired acid doping level and the proton conduction, through differentiations in the chain conformations or the phase separation in the presence of phosphoric acid. Other influencing factors can be the rigidity of the structure and the intermolecular bonds. Moreover, in the case of cross-linked materials, the doping ability and proton conductivity are further strongly influenced not only by the cross-linking density, but also by the chemistry used and the nature of the formed "bridges" between the polymer chains, as will be discussed further in the next section. It should be stated that for each material there is an optimum range of acid uptake combining high conductivity values and good mechanical properties in order to be used in PEMFCs.

A vast literature has been devoted to the study of the proton conduction and the effect of relative humidity on the conductivity of the polymer/phosphoric acid systems [39, 43–48]. The conduction mechanism is substantiated through the proton transfer between a proton donor and a proton acceptor in combination to the ability of the proton carrier (positive ion) to rotate and move so that it will transfer the proton. Proton conductivity increases with relative humidity at a given temperature because the higher water content in the electrolyte lowers the viscosity within the membrane leading to higher mobility and rendering it more conductive [43], while it can play the role of proton carrier itself and provide more pathways (Hydrogen bonds) for protons to hop. Water molecules can play a significant role in the configurational proton transfer through the H_3PO_4 imbibed polymer electrolytes as they are flexible to move, rotate, and be aligned with H_3PO_4 so that the hoping of H^+ can be facilitated. Moreover, according to calculations of the H–O bond distances, hydrogen bond between water and phosphoric acid has the longest distance (and thus weaker hydrogen bond) allowing a high degree of mobility and rotation, in comparison to hydrogen bonds of other species [39]. In this respect, the equilibrium water content is critical for the improvement of membrane's proton conductivity. The physicochemical interactions of water vapors with the polymer electrolyte and the promoting effect on the fuel cell performance were also proven [36]. The relative humidity dependence on conductivity is much greater in low temperature water-based systems like Nafion than in acid-based electrolytes [46]. For an acid-doped electrolyte, the conductivity dependence on relative humidity is more pronounced as temperature increases [43]. The conductivity of acid-doped PBI with a doping level of 560 mol% increases from 3.8 to 6.8×10^{-2} S cm^{-1} at 200 °C with an increase in the relative humidity from 0.15 to 5 % [46, 49]. Moreover, for a PBI/**Copolymer II** blend with a wet phosphoric acid doping level of 220 wt%, conductivity increases from 2.7 to 8.6×10^{-2} S cm^{-1} at 170 °C with an increase in the steam partial pressure from 1 to 10 kPa (relative humidity 0.127 and 1.27 %, respectively) [42].

5.5.1 Equilibrium Hydration Levels of Water in the H_3PO_4 Imbibed Membranes

The equilibrium hydration level depends both on temperature and on steam partial pressure. The water generated at the cathode and the extent to which it equilibrates in the membrane may vary between the different polymer electrolytes, their acid doping level, and the preparation method of the electrolyte, e.g., the solvent used for the

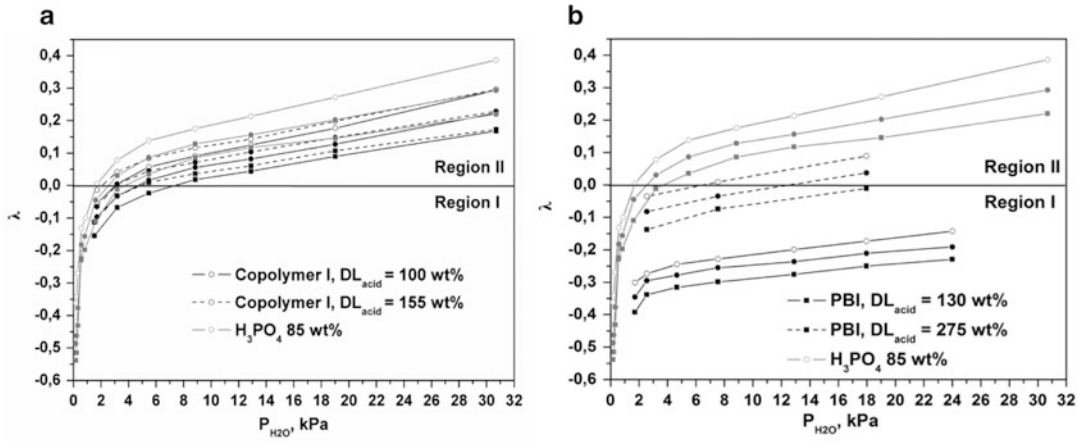

Fig. 5.14 The effect of water vapor partial pressure (P_{H_2O}) on the hydration level of acid-doped (**a**) **Copolymer I** and (**b**) PBI at different acid doping levels at 150 °C (*open circles*), 160 °C (*solid circles*), and 170 °C (*squares*). The corresponding results with H_3PO_4 85 wt% (*grey lines*) are also plotted for comparison. Reproduced from [37] with permission of the Royal Society of Chemistry

casting may determine the free volume expansion and therefore the solubility coefficient of water. The electrolyte affinity to water is of special importance, not only because water can affect the proton conduction, but also due to the possibility of acid dilution (temperature shutdown) or electrolyte redistribution due to volume expansions/contractions (especially during start/stop cycling), which can lead to long-term loss in conductivity or the membrane stability. A series of temperature programmed thermogravimetric (TGA) experiments under controlled humidified atmosphere shed light to the structural effect on water affinity and retention [37]. Two different state-of-the-art high temperature polymer electrolyte structures were used, **Copolymer I** [10] and standard m-PBI, while liquid H_3PO_4 85 wt% was used for comparison.

When temperature increases under dry atmosphere the following sequential processes take place:

- At temperatures below 100 °C, free water is evaporated leaving dry phosphoric acid in the polymer matrix.
- Further increase of the temperature leads to additional water evaporation as a result of the dehydration of H_3PO_4 and the formation of $H_4P_2O_7$ according to reaction (5.1) and in general the polymerization reaction (5.2) at even higher temperatures. Despite the fact that pyrophosphoric acid is a strong acid, its formation is accompanied by the significant decrease of the fuel cell performance due to the decrease of mobility, as well as the ionic capacity (i.e., two molecules of phosphoric are substituted by one molecule of pyrophosphoric acid).

$$2H_3PO_4 = H_4P_2O_7 + H_2 \quad (5.1)$$

$$nH_3PO_4 = H_{2n-2}P_nO_{2n-1} + (n-1)H_2O \quad (5.2)$$

When the samples are exposed to humidity, water is being adsorbed. In Fig. 5.14, the hydration level of different acid-doped **Copolymer I** and PBI systems is depicted varying the temperature and humidity [37]. The hydration level is expressed through the dimensionless parameter, lambda (λ), which corresponds to the number of water molecules associated with one orthophosphoric acid molecule and is calculated according to (5.3)–(5.5), where W_{pol} is the weight of the undoped material, MW corresponds to the respective molecular weight of water and of H_3PO_4, $W_{H_3PO_4}$ is the weight of the dry acid imbibed upon doping of the polymers, W is the recorded weight, W_{H_2O} is the weight of water

absorbed upon exposure of the sample to humidified gases during the experiment, and W_{ref} is a reference weight where the free water is evaporated from the acid/polymer system.

$$W_{H_3PO_4} = W_{ref} - W_{pol} \tag{5.3}$$

$$W_{H_2O} = W - W_{ref} \tag{5.4}$$

$$\lambda = mol_{H_2O}/mol_{H_3PO_4} = (W_{H_2O} \times MW_{H_3PO_4})/(W_{H_3PO_4} \times MW_{H_2O}) \tag{5.5}$$

Two processes take place. Water is absorbed due to the hydrolysis of the pyrophosphoric acid according to the reverse of (5.1), up to the point that $\lambda = 0$, showing that the dimerization of phosphoric acid is a fully reversible process. As expected, the equilibrium constant of phosphoric acid dimerization increases with temperature. Further increase in P_{H_2O} resulted in solubility of free water in the H_3PO_4/polymer system. There is a similar dependence on P_{H_2O} for all samples used; sharp increase at low P_{H_2O} and thereafter linear variation of λ. An increase of the acid doping level of the polymers results in enhanced ability to absorb water.

The chemical structure strongly influences the thermodynamics of the hydration process of the imbibed acid and therefore the ability of the electrolyte to absorb water molecules from steam. For similar acid contents, doped **Copolymer I** has a higher ability to absorb water than acid-doped PBI. Even at the low initial acid doping levels of 100 wt%, the behavior of acid imbibed **Copolymer I** is closer to that of phosphoric acid, denoting that the interactions of acid with this matrix are not strong or extended enough to disturb the network of the acid and alter its physicochemical properties. By exposing the sample to only 2–3 kPa of water, depending on the doping level at 150 °C all acid is in the orthophosphoric form. On the other hand, acid-doped PBI inhibits the reversion of reaction (5.1) and absorbs less water reflecting a difference on the physicochemical interactions of the acid inside the two matrixes. The stronger basic character of the imidazole group, along with the formation of the stronger pyrophosphoric acid upon dehydration leads to electrolytes with smaller affinity to water. Equilibrium isotherms at various water content over a range of temperatures from 30 to 180 °C using Celtec®-P Series 1000 MEAs also prove this behavior [50]. In the temperature range between 160 and 180 °C, positive values of the hydration level (λ) were only obtained for water partial pressures above 20 kPa. Note that Celtec®-P electrolytes are polymer gels containing PBI and phosphoric acid with high phosphoric acid contents of more than 95 wt% or up to 70 phosphoric acid molecules per PBI repeat unit [51].

Similar reports on the affinity of PBI/phosphoric acid systems to water exist. Schechter et al. [52] showed that water is absorbed in the polymer under different water activity and it interacts with phosphorous species changing the concentration of the mobile acid in a similar way to liquid acid, using a series of ^1H and ^{31}P liquid probe NMR measurements under carefully controlled humidity. Li et al. [53] examined the relationship between phosphoric acid doping level and water uptake. For pristine PBI membranes and PBI membranes with low acid doping levels (<200 mol%) the water uptake is small. In fact, the water uptake from the vapor phase for PBI with a doping level 170 mol% was found to be lower than that for the pristine PBI, attributed to the fact that the active sites of the imidazole ring are preferably occupied by the acid molecules. A more significant increase was observed for the membranes with high doping acid levels, indicating that this water uptake is associated with the acid doping level. At high acid doping levels, water uptake of m-PBI at room temperature was comparable to or even exceeded that of the commercially available Nafion in the high humidity range.

5.5.1.1 Stability and Volatility of H_3PO_4 in the Imbibed Membranes

The stability and volatility of H_3PO_4 in the polymer matrix was studied by a set of long-term TGA experiments under humidified conditions. Representative examples are presented in

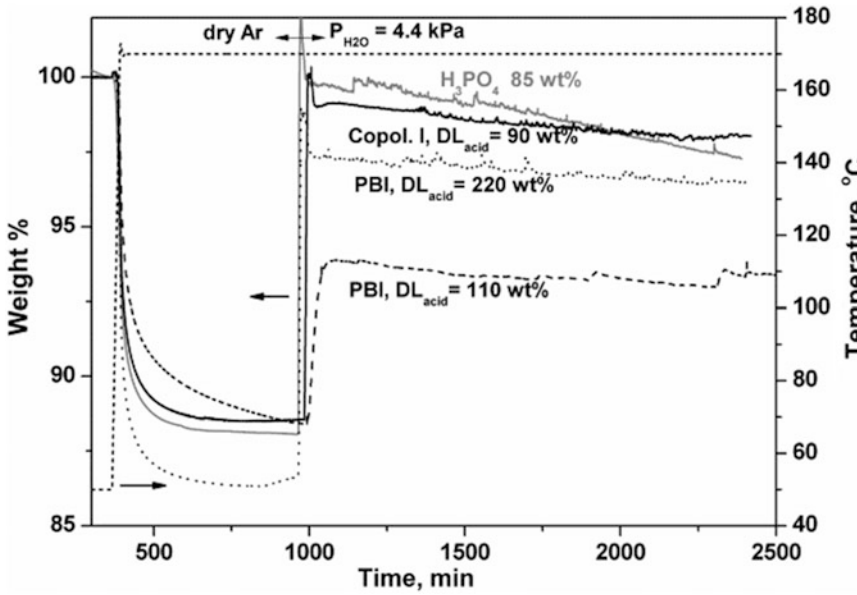

Fig. 5.15 Thermogravimetric analysis of H_3PO_4 and acid-doped **Copolymer I** and PBI under dry and humidified atmosphere, $P_{H_2O} = 4.4$ kPa. The dry argon flow rate was 150 cm^3/min. The contribution of the polymer matrix has been subtracted. The weight of all samples has been normalized considering that 100 wt% is the initial weight of the dry acid, $100(W_{ref} - W_{pol})/W_{ref} = 100$ wt%. Reproduced from [37] with permission of the Royal Society of Chemistry

Fig. 5.15 for H_3PO_4 and acid-doped **Copolymer I** & PBI. Initially, all samples were equilibrated under dry Ar atmosphere at 50 °C. Upon temperature increase to 170 °C, the weight decreased due to acid dehydration. Thereafter, a certain water partial pressure was introduced over the samples (4.4 kPa for the examples in Fig. 5.15) and was kept constant for a relatively long period in order to record the stability of the system and evaluate the rate of evaporation of phosphoric acid itself. As also stated earlier, doped **Copolymer I** and liquid phosphoric acid almost recover their initial weight at 50 °C, reversing the dehydration reaction (5.1). On the contrary, PBI does not reach W_{ref} even for 220 wt% acid doping level. In [37] the weight loss rate or else the normalized evaporation rate of the H_3PO_4 for several samples and different vapor partial pressures is reported and was concluded that:

1. An increase in evaporation rate is observed upon increasing steam partial pressure and/or acid doping level.
2. The evaporation rate of H_3PO_4 from **Copolymer I** is approximately 60 % higher than the corresponding rate from the PBI membrane being at the same H_3PO_4 doping level, in accordance to the weaker interaction of the acid with **Copolymer I**, leading to a behavior closer to H_3PO_4. In any case, the use of a polymer matrix compared to plain phosphoric acid can decrease the evaporation rate even by a factor of 3. The differentiation between the three systems is closely related to modifications in the physicochemical properties of the H_3PO_4 through its interactions with the polymer matrix.

5.5.2 Steam Permeability Through the Membrane

Using in situ experimental protocols, it has been explicitly proven that the steam permeates through the membrane electrolyte. Given the fact that other gases smaller in the size of their molecules cannot penetrate the electrolyte at comparable high rates as water, the crossover mechanism of steam cannot be interpreted by considering a diffusion process through the void

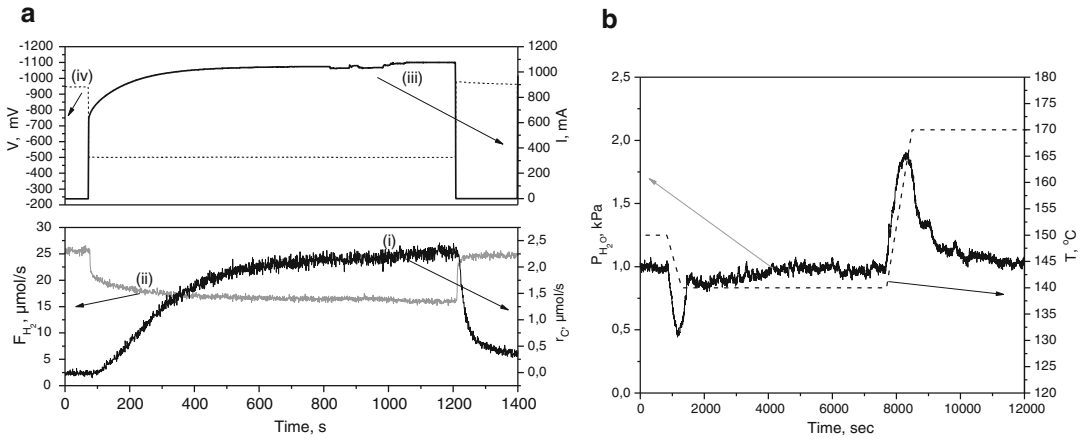

Fig. 5.16 (**a**) The transient evolution of (*i*) H_2O and (*ii*) H_2 flow rates at the anode outlet and (*iii*) current *I* upon (*iv*) voltage application of $V_{cell} = -0.5$ V. The anode/cathode feed gas composition was dry H_2 30 %–Ar/O_2; (**b**) H_2O evolution during the stepwise variation of the reactor's temperature. The feed gas composition to both compartments of the cell is 1 mol% H_2O/He mixture. Electrolyte: PBI/**Copolymer II** 50/50. Doping level: 200 wt%. Membrane thickness: 70 μm. Reproduced from [36] with permission of Elsevier

volume of the polymer membrane. Taking into consideration that permeability through a membrane is defined by (5.6) [54], it has been proposed that the high permeation rate of water is because of the high solubility of water in phosphoric acid and its chemical interaction with pyrophosphoric acid according to reverse of reaction (5.1) [36].

$$P(\text{permeability}) = S(\text{solubility in electrolyte}) \times D(\text{diffusivity in electrolyte}) \tag{5.6}$$

Though water vapor plays a significant role in conductivity and therefore fuel cell performance, the humidification of H_2 and O_2 is not necessary. The water vapors produced from the electrochemical reaction at the cathode compartment penetrate through the polymer electrolyte to the anode compartment. Upon this back-transport process, the electrolyte is being hydrated with a direct positive effect on the fuel cell performance. This has been shown under real fuel cell operating conditions, Fig. 5.16a [36]. The transient evolution of the anode gases concentration was recorded upon cell potential application of 500 mV. On fuel cell operation, hydrogen is progressively consumed approaching steady state, while the water signal is observed to increase approaching a constant value. Therefore, the produced water can penetrate and evolve at the anode compartment. In addition, the transient evolution of the water signal is followed by the corresponding increase in hydrogen conversion and cell current, thus indicating the direct effect of water transport through the membrane on the fuel cell performance. Figure 5.16b depicts a temperature variation in situ experiment showing that the acid-doped electrolyte membrane absorbs and retains varying amounts of water at different temperatures. Both compartments were fed with Ar–1% H_2O mixture at 150 °C. Upon stepwise decrease or increase of cell's temperature, water is being observed to be absorbed or to be evolved from the membrane, respectively. This shows that varying equilibrium water/MEA conditions are established at different temperatures.

5.6 Application in HT-PEMFCs Operating up to 220 °C

The aromatic polyethers bearing pyridine moieties described in the previous sections have been effectively used as polymer electrolytes in fuel cells. Because of the use of several different

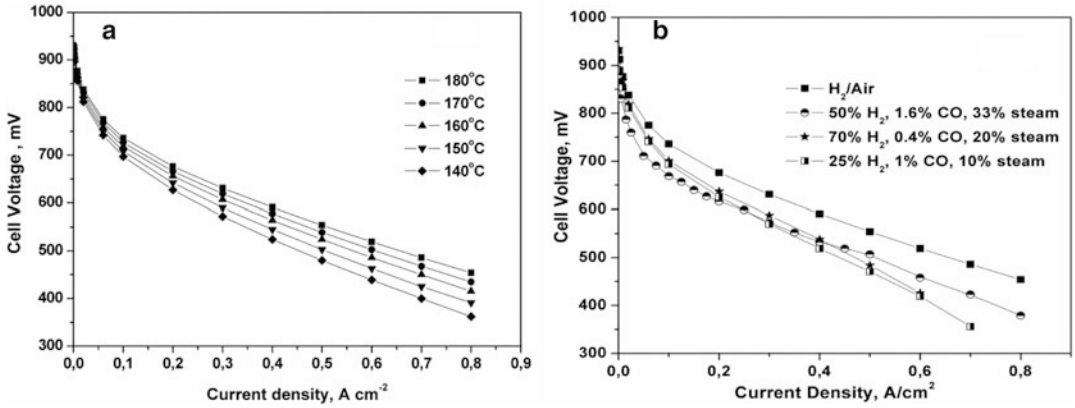

Fig. 5.17 *I–V* curves of MEA based on **Copolymer IX**, (**a**) with H_2 and air feeds (λH_2: 1.2, λ_{air}: 2.0) and (**b**) different reformate/air feeds at ambient pressure. Active surface area = 25 cm^2

membranes as electrolytes, it was not feasible to find the optimum conditions for each one, since several parameters regarding the design, construction, and assembling of the membrane electrode assembly (MEA) must be taken into account in order to have optimum performance. It should not be neglected that commercialization of PEMFCs is still restricted by its high cost since noble metals are typically used as electrocatalysts. Reduced cost, resulting from increased catalyst utilization and/or catalyst stability, is highly desirable. The design of electrodes for PEMFCs is a delicate balancing of transport media. Transport of gases and conductance of electrons and protons to the electrochemical interface must be optimized to provide efficient electrochemical reactions [55]. In this respect, for this type of cells, increase of the triple-phase boundaries has been attempted by developing a new type of Pt/carbon nanotubes (Pt/CNTs)-based electrocatalysts, where the carbon substrate, following the pattern of the electrolyte, is chemically functionalized with polar pyridine groups, which are expected to interact with phosphoric acid, secure the uniform distribution of the acid throughout the catalytic layer, and provide a 3D proton ionic link with all deposited Pt particles [56–58]. In the present discussion, focus will be paid on the electrochemical characterization of the polymer electrolytes discussed. Certainly, in most cases, optimization of the MEA construction and operational parameters will further enhance the performance. The electrochemical characterization will be confined on their fuel cell performance and stability.

5.6.1 Linear Polymeric Membranes

The linear polymeric materials have shown excellent performance and stability operating up to 180–200 °C [59]. An example of the cell performance obtained for this category of polymer electrolytes is given in Fig. 5.17, where the polarization curve of a fuel cell operating at 140–180 °C using hydrogen and air dry gases with stoichiometric flow rates at anode and cathode is depicted. The durability of these systems is presented in Fig. 5.18, where a long-term fuel cell stability test under steady state operation at 0.22 A cm^{-2} and different feed gases is depicted.

It should be noted here that besides the initial syntheses and studies of the linear copolymers, a lot of effort for the optimization of selected copolymers' preparation in terms of composition control and molecular weight increase together with MEA construction and testing has been devoted by the spin-off company Advent S.A. [60].

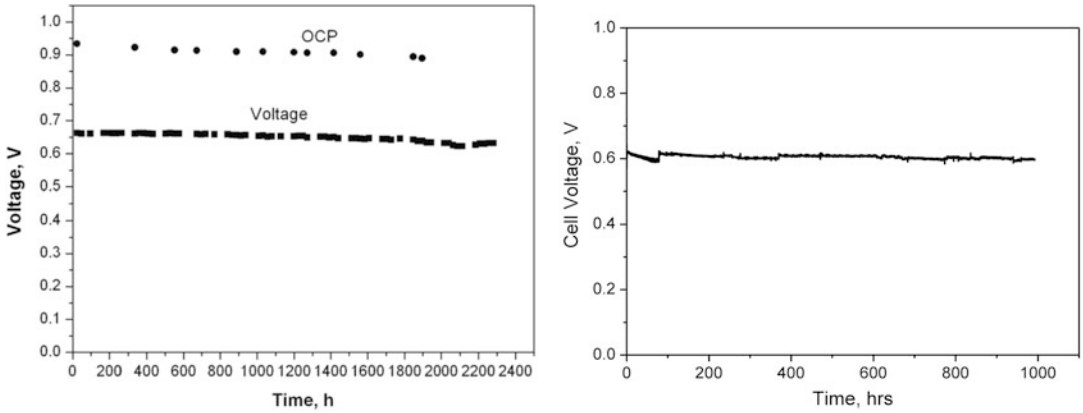

Fig. 5.18 Fuel cell stability test for **Copolymer IX** at 180 °C and ambient pressure. (**a**) Anode: H_2 ($\lambda = 1.2$), cathode: air ($\lambda = 2$) and (**b**) anode: 71.3 % H_2 ($\lambda = 1.3$), 2.1 % CO, 26.6 % CO_2, cathode: air ($\lambda = 2.2$)

5.6.2 Cross-Linked Membranes

A critical issue of all the aforementioned linear polymer electrolytes is the deficient long-term durability of these systems at temperatures well above 180 °C. Over 5000 h for vehicles and 40,000 h for stationary applications are the required life times of PEMFCs [61]. At the same time, increasing the fuel cells operation temperature even above 180 °C offers several distinct advantages like increased conductivity of the acid-doped membranes at lower doping levels, increased tolerance of the catalytic layers to contaminants, better heat management and heat utilization and efficient combination with other electrochemical devices, e.g., a methanol or liquid petroleum gas (LPG) reformers. This target requires modifications in the chemical structure of the standard membranes towards the increase of intermolecular interactions. The challenge is to develop materials with increased mechanical stability, but with adequate ionic conductivities. Post-polymerization cross-linking by covalent bonding between the macromolecules has the strongest and more permanent impact on the polymer structure and is thoroughly described in the previous sections of this chapter. In brief, side cross-linkable groups were introduced on the chemical structure like carboxylic acid [27], propenyl [24], or styryl [26] groups. Post-polymerization covalent cross-linking (thermal, covalent with the use of cross-linkers or covalent in acid [25]) improved the mechanical properties in terms of glass transition temperature. Different chemistries were explored and resulted in materials with differentiations in the properties, as well as their fuel cell performance.

Conductivity of the linear and cross-linked materials with the carboxylic acid functionalities (**Copolymers XII** and **XXII**) was evaluated in situ by means of AC impedance spectroscopy as shown in Fig. 5.19a. For all materials, the conductivity exceeded the value of 8×10^{-2} S cm^{-1} and in some cases reached 10^{-1} S cm^{-1} above 180 °C. As expected, temperature increase improved the ionic conductivity. The cross-linked material depicted lower conductivity values compared to its linear counterpart at the same doping levels. In the case of the cross-linked material, this doping level is not the maximum that can be achieved; therefore this drawback can be compensated by increasing the doping level. The non-cross-linked materials showed high performance and good stability at temperatures up to 180 °C [27]. Above that temperature the performance of the corresponding MEAs slowly deteriorated. As explained above, two cross-linking methods were investigated for the cross-linking of **Copolymers XII** and **XXII**, the dihydrazine (TDH) and the bistetrazole (BTT) routes toward the formation of oxadiazole bridging moieties. The cross-linked membranes

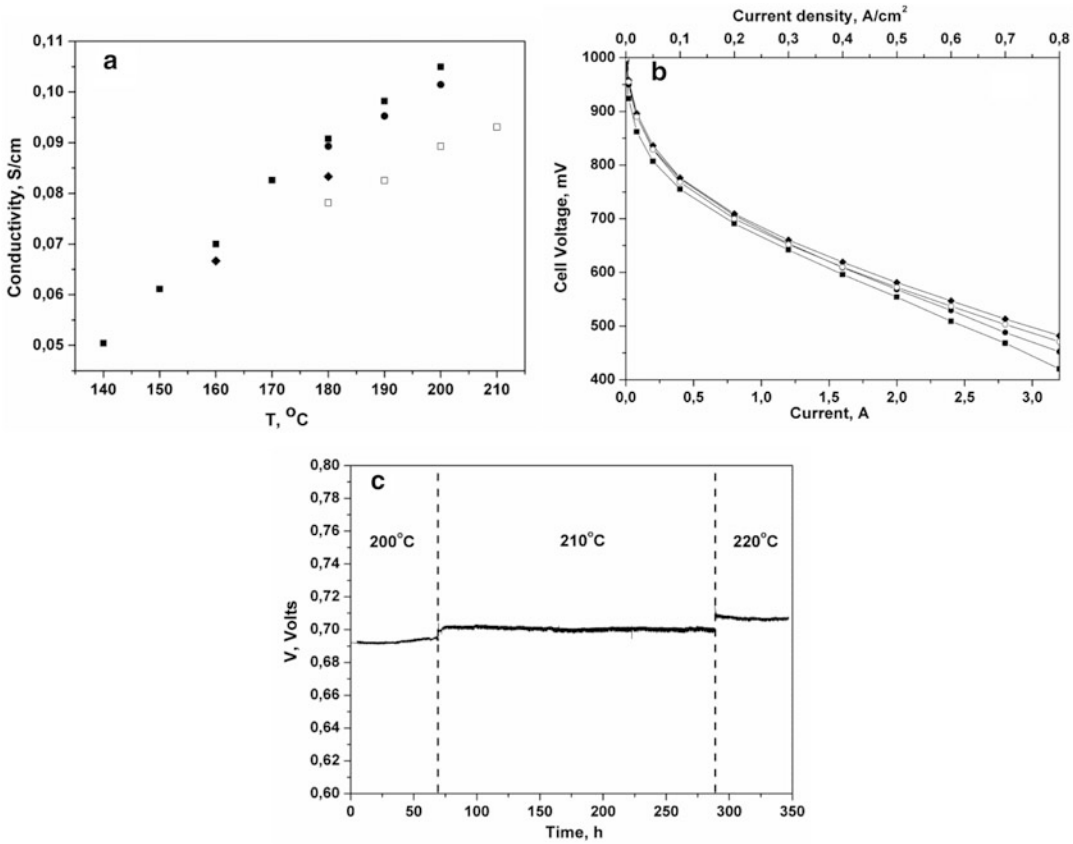

Fig. 5.19 (**a**) Temperature dependence of ionic conductivity of **Copolymer XXII** ($x = 70$, $z = 10$) with DL = 193 % and thickness 110 μm (*filled square*) and with DL = 170 % and thickness 160 μm (*filled diamond*); of **Copolymer XII** ($x = 70$, $z = 20$) with DL = 200 % and thickness 125 μm (*filled circle*); and of the cross-inked **Copolymer XII$_{CL\text{-}BTT(100)}$** ($x = 70$, $z = 10$) with DL = 210 % and thickness 175 μm (*open square*). Conductivities measured at 0.2 A cm^{-2} using dry gases with hydrogen and oxygen (stoichiometric ratio of 1.2 and 2, respectively) at ambient pressure. (**b**) Current–voltage curves at 200 °C (*filled square*), 210 °C on the 5th (*filled circle*) and 15th (*open circle*) day of operation and 220 °C (*filled diamond*) and (**c**) cell potential versus time at 0.2 A cm^{-2} and at several operating temperatures between 200 and 220 °C. For (**b**) and (**c**), the MEA was based on the cross-linked **Copolymer XII$_{CL\text{-}BTT(100)}$** ($x = 70$, $z = 10$). Active area: 4 cm^2. Dry gases with hydrogen and oxygen (stoichiometric ratio of 1.2 and 2, respectively) at ambient pressure. Reproduced from [27] with permission of the Royal Society of Chemistry

through BTT were superior and MEAs were therefore formulated. Initial electrochemical characterization showed very promising results. Figure 5.19b depicts the polarization curves at temperatures up to 220 °C for the MEA based on the cross-linked **Copolymer XXII$_{CL\text{-}BTT(100)}$** using dry gases H_2/O_2 (anode/cathode) with stoichiometric ratio. The fuel cell performance is improved with increasing temperature due to the increased ionic conductivity of the electrolyte and the enhanced reaction kinetics. Potential values $V = 697$, 703, and 712 mV were obtained at 0.2 A cm^{-2} at ambient pressure and at 200, 210, and 220 °C, respectively. A short stability evaluation test is presented in Fig. 5.19c, showing stable performance with no sign of degradation for at least 350 h at operational temperatures between 200 and 220 °C.

Another example of a chemically cross-linked material is the case of polymers containing cross-linkable propenyl groups cross-linked with the use of a bisazide [24]. Figure 5.20a depicts the

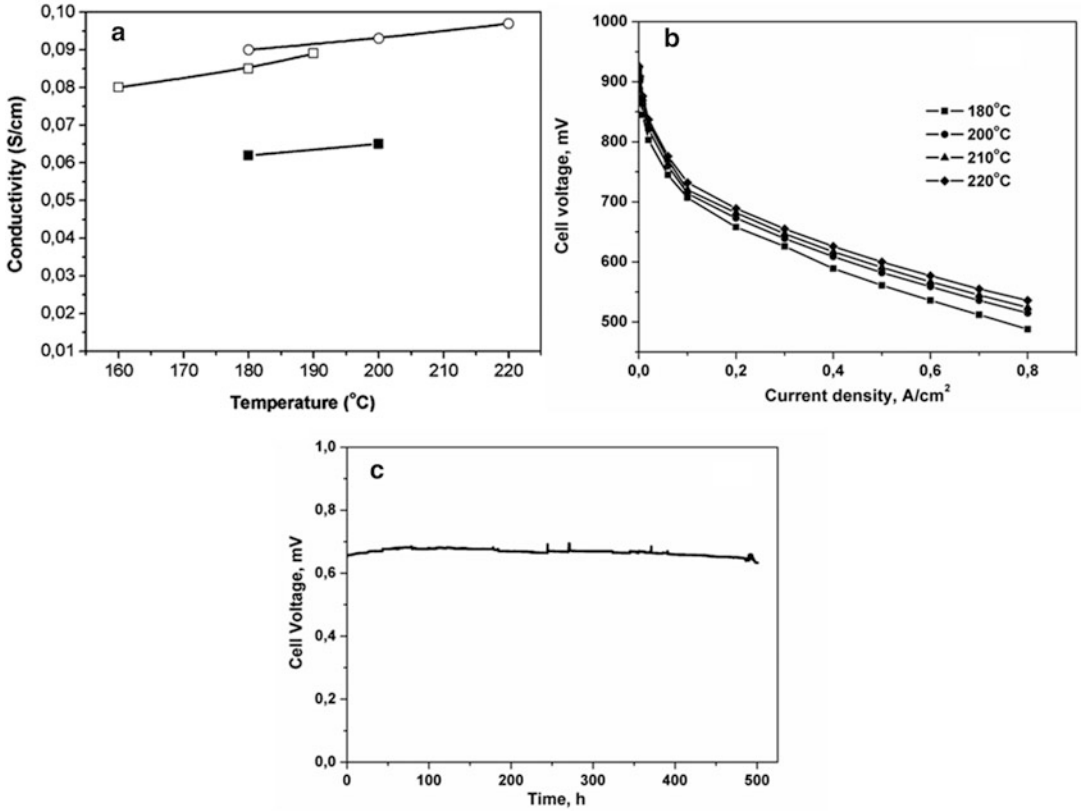

Fig. 5.20 (**a**) Temperature dependence of ionic conductivity for the **Copolymer XVII** ($x = 75$) with $DL_{acid} = 160$ wt% (*filled square*) **Copolymer XVII$_{CL}$** ($x = 75$) with $DL_{acid} = 140$ wt% (*open square*) and **Copolymer XVII$_{CL}$** ($x = 70$) with $DL_{acid} = 195$ wt% (*open circle*). Membrane thicknesses: 140, 120, and 110 μm, respectively. Reproduced from [24] with permission of the American Chemical Society; (**b**) current–voltage curves at temperatures 180–220 °C; (**c**) long-term stability measurements at 210 °C and 0.2 A cm^{-2} of a cross-linked MEA using the **Copolymer XX$_{CL}$**. $DL_{acid} = 320$ wt%. Active area 25 cm^2. Feed: H_2/air 1.2/2.0

temperature dependence of the ionic conductivity for the MEAs which were formed from the cross-linked membranes and the azide-free polymer. It must be noticed that although the cross-linked and non-cross-linked membranes absorbed almost the same quantity of acid, the conductivity of the cross-linked one is slightly higher compared to the neat polymer. This fact is in agreement with previous studies related to the effect of the polymeric structure on the conductivity. In the cross-linked structure, the presence of the aziridines or amines not only increases the materials doping ability, but the conductivity as well. It should be mentioned that although the cross-linking is known to decrease the ionic conductivity, in this case the selected cross-linker created functional groups which provided more pathways for the proton transfer and subsequently higher conductivity values were noticed. The performance of the MEA comprising the aforementioned covalently cross-linked membrane can be seen in Fig. 5.20b, while as presented in Fig. 5.20c it showed stable operation at 210 °C for 500 h at 0.2 A cm^{-2} with H_2/Air feed. The cell voltage is 660 mV and the corresponding power density is 0.132 W cm^{-2}. Over the course of the experiment the average voltage drop was only 3 μV h^{-1}. This provides evidence for their high chemical, thermal, and oxidative stability.

In an attempt to simplify the cross-linking procedure, thermal cross-linking of polymers bearing side styryl double bonds are reported

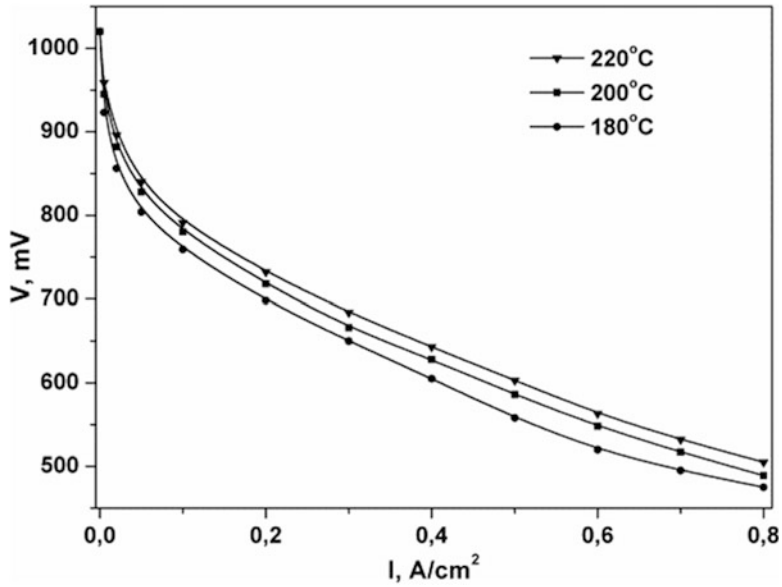

Fig. 5.21 Current–voltage curves for the cross-linked **Copolymer XXI$_{CL}$** ($x + z = 60$, $z + w = 15$)-based MEA at several operating temperatures using dry H_2/O_2 gases ($\lambda = 1.2$ and 2, respectively) at ambient pressure. $DL_{acid} = 160$ wt%, active area: 4 cm^2. Reproduced from [26] with permission of Elsevier

[26]. The properties of the virgin materials allowed heating above their glass transition temperature (at 250 °C) where the double bonds become reactive and are able to cross-link without the use of thermal initiators or cross-linking agents. Unfortunately, the doping ability in phosphoric acid was decreased, as is common upon the formation of more compact structures. Despite the moderate phosphoric acid doping levels, in situ conductivity reached values above 5×10^{-2} S cm^{-1}. Preparation of MEAs and preliminary fuel cell tests gave a very promising performance. The polarization curves are shown in Fig. 5.21. Cross-linking allowed measurements up to 220 °C demonstrating the enhanced stability and their feasibility to be used in high temperature PEM fuel cells.

As explained previously, cross-linking during the impregnation of the membranes (bearing propenyl groups) in phosphoric acid remarkably simplifies the whole procedure, while at the same time leads to materials with enhanced ability to absorb and retain high amounts of phosphoric acid without losing their mechanical integrity [25]. As a result of the increased acid uptakes, in situ measurements by means of AC impedance spectroscopy revealed the high conductivity values obtained, Fig. 5.22a, in most cases in the order of 10^{-1} S cm^{-1}. The advanced cross-linked membranes were tested in single cells operating at high temperatures up to 220 °C, Fig. 5.22b. A durability measurement at steady state operation at 0.2 A cm^{-2} at 210 °C is shown in Fig. 4.22c. The promising performance and stable operation in combination with and the simplified technique used for their preparation demonstrate the feasibility of these electrolytes to be used in high temperature PEM fuel cells operating well above 180 °C.

5.7 Conclusions

Taking advantage of the possibilities offered by polymer chemistry for creating novel materials, a new generation of polymeric membranes for HT-PEM fuel cells has been designed and developed. The herein presented aromatic polyether sulfones carrying main chain pyridine units have been proven to be a reliable polymer electrolyte material for the HT-PEM fuel cell technology. These materials exhibit certain

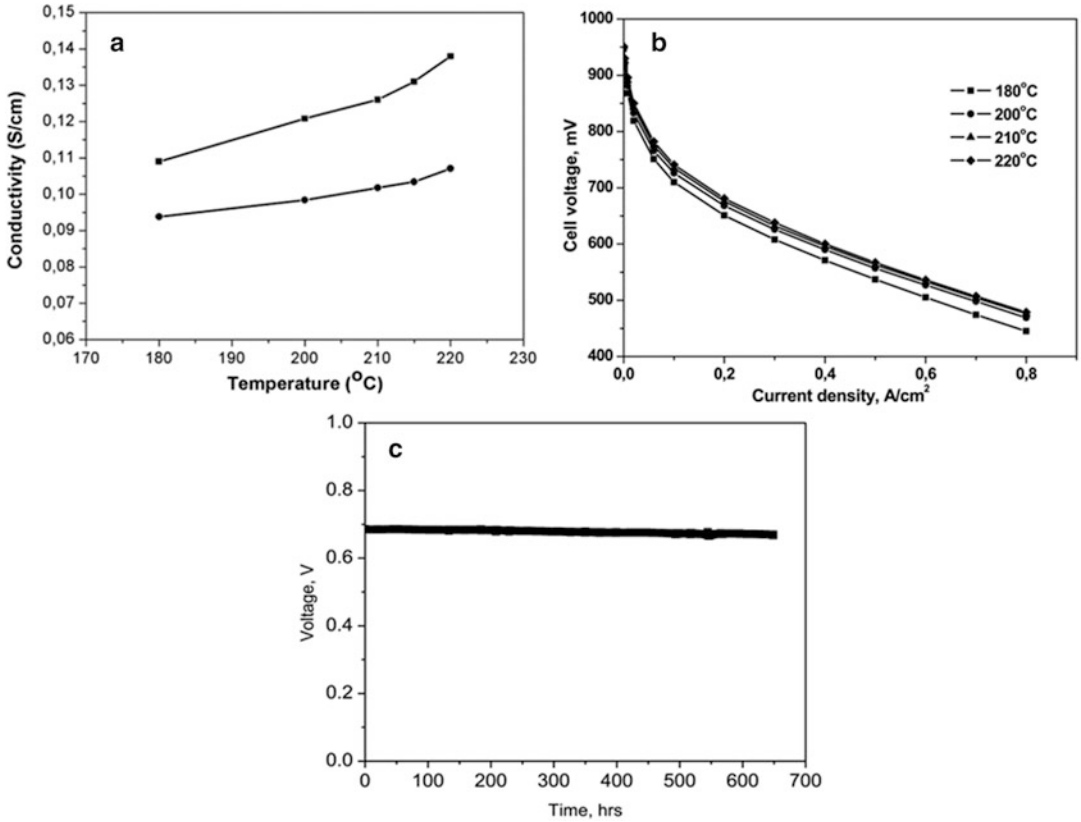

Fig. 5.22 (**a**) Temperature dependence of ionic conductivity for the cross-linked in acid **Copolymer $\mathbf{XX_{CL\text{-}acid}}$** with $DL_{acid} = 280$ wt% (*filled circle*) and 350 wt% (*filled square*). Reproduced from [25] with permission of Elsevier; (**b**) current–voltage curves of a **Copolymer $\mathbf{XX_{CL\text{-}acid}}$**-based MEA with $DL_{acid} = 350$ wt% at several operating temperatures using dry H_2/O_2 gases ($\lambda = 1.2$ and 2, respectively); (**c**) long-term stability measurement of **Copolymer $\mathbf{XX_{CL\text{-}acid}}$**-based MEA at 210 °C and 0.2 A cm^{-2} at ambient pressure. $DL_{acid} = 208$ wt%, active area: 25 cm^2

advantages as compared to PBI polymer electrolytes with regards to their manufacturing properties, their operating conditions, and their performance characteristics. These comprise their very good film-forming properties, thin robust membranes with long lasting mechanical and chemical stability, adequate proton conductivity ($0.8–1 \times 10^{-1}$ S cm^{-1}) and operating temperatures ranging between 170 and 210 °C. The latter widens its technological applications so that advanced compact engineering design of fuel cell systems allows either the use of diversity of fuels or the operation of the fuel cell stack within a wide span of temperatures providing sustainable operation under dynamic load. In particular, the MEA operation at 210 °C allows for the effective integration of a methanol reformer in the HT-PEM fuel cell stack, thus resulting into a compact simple and versatile fuel cell system especially for portable applications.

Acknowledgements Financial support from European Commission and from the Fuel Cell and Hydrogen Joint Undertaking (FCH JU) is greatly acknowledged. The authors are also indebted to Advent SA personnel for their collaboration.

References

1. Li QF, Jensen JO, Savinell RF et al (2009) High temperature proton exchange membranes based on polybenzimidazoles for fuel cells. Prog Polym Sci 34:449–477
2. Bouchet R, Siebert E (1999) Proton conduction in acid doped polybenzimidazole. Solid State Ionics 118:287–299
3. Kim SK, Kim TH, Ko T et al (2011) Cross-linked poly (2,5-benzimidazole) consisting of wholly aromatic groups for high-temperature PEM fuel cell applications. J Membr Sci 373:80–88
4. Asensio JA, Borros S, Gomez-Romero P (2004) Proton-conducting membranes based on poly (2,5-benzimidazole) (ABPBI) and phosphoric acid prepared by direct acid casting. J Membr Sci 241:89–93
5. Kim HJ, Cho SY, An SJ et al (2004) Synthesis of poly (2,5-benzimidazole) for use as a fuel-cell membrane. Macromol Rapid Commun 25:894–897
6. Yu S, Benicewicz BC (2009) Synthesis and characterization of functionalized polybenzimidazoles for high temperature PEMFC's. Macromolecules 42: $32#8640–8648
7. Gourdoupi N, Andreopoulou AK, Deimede V et al (2003) A novel proton conducting polyelectrolyte composed of an aromatic polyether containing main-chain pyridine units for fuel cells applications. Chem Mater 15:5044–5050
8. Andreopoulou AK, Kallitsis JK (2002) From terphenyl-dendronized macromonomers to aromatic-aliphatic polyethers bearing two pendant dendrons per repeating unit. Macromolecules 35:5808
9. Gourdoupi N, Papadimitriou K, Neophytides S et al (2008) New high temperature polymer electrolyte membranes. Influence of the chemical structure on their properties. Fuel Cells 8:200–208
10. Pefkianakis EK, Deimede V, Daletou MK et al (2005) Novel polymer electrolyte membrane, containing pyridine and tetramethyl biphenyl units, for application in high temperature PEM fuel cells. Macromol Rapid Commun 26:1724–1728
11. Geormezi M, Deimede V, Gourdoupi N et al (2008) Novel pyridine-based poly(ether sulfones) and their study in high temperature PEM fuel cells. Macromolecules 41:9051–9056
12. Daletou MK, Geormezi M, Pefkianakis EK et al (2010) Fully aromatic copolyethers for high temperature polymer electrolyte membrane fuel cells. Fuel Cells 10:35–44
13. Daletou MK, Gourdoupi N, Kallitsis JK (2005) Proton conducting membranes based on PBI/polysulfone copolymer blends. J Membr Sci 252:115–122
14. Hubner G, Roduner E (1999) EPR investigation of HO radical initiated degradation reactions of sulfonated aromatics as model compounds for fuel cell proton conducting membranes. J Mater Chem 9:409–418
15. Kerres J, Schönberger F, Chromik A et al (2008) Partially fluorinated arylene polyethers and their ternary blend membranes with PBI and H_3PO4. Part I. Synthesis and characterisation of polymers and binary blend membranes. Fuel Cells 8:175–187
16. Kallitsis JK, Geormezi M, Neophytides S (2009) Polymer electrolyte membranes for high temperature fuel cells based on aromatic polyethers bearing pyridine units. Polym Int 58:1226–1233
17. Deimede V, Voyiatzis GA, Kallitsis JK et al (2000) Miscibility behavior of polybenzimidazole/sulfonated polysulfone blends for use in fuel cell applications. Macromolecules 33:7609–7617
18. Geormezi M, Chochos CL, Gourdoupi N et al (2011) High performance polymer electrolytes based on main and side chain pyridine aromatic polyethers for high and medium temperature PEM fuel cells. J Power Sources 196:9382–9390
19. Andreopoulou AK, Daletou MK, Kalamaras I et al (2012) Crosslinked or non-crosslinked aromatic (co)polymers as proton conductors for use in high temperature PEM fuel cells. US Patent Application No. 13367855/02.07.2012
20. Morfopoulou C, Andreopoulou AK, Kallitsis JK (2011) The effect of structural variations on aromatic polyethers for high temperature PEM fuel cells. J Polym Sci A Polym Chem 49:4325–4334
21. Papadimitriou KD, Andreopoulou AK, Kallitsis JK (2010) Phosphonated fully aromatic polyethers for PEMFCs applications. J Polym Sci A Polym Chem 48:2817–2827
22. Kalamaras I, Daletou MK, Gregoriou VG et al (2011) Sulfonated aromatic polyethers containing pyridine units as electrolytes for high temperature fuel cells. Fuel Cells 11:921–931
23. Voege A, Deimede VA, Kallitsis JK (2012) Side chain crosslinking of aromatic polyethers for high temperature polymer electrolyte membrane fuel cell applications. J Polym Sci A Polym Chem 50:207–216
24. Papadimitriou KD, Paloukis F, Neophytides SG et al (2011) Cross-linking of side chain unsaturated aromatic polyethers for high temperature polymer electrolyte membrane fuel cell applications. Macromolecules 44:4942–4951
25. Papadimitriou KD, Geormezi M, Neophytides SG et al (2013) Covalent cross-linking in phosphoric acid of pyridine based aromatic polyethers bearing side double bonds for use in high temperature polymer electrolyte membrane fuel cells. J Membr Sci 433:1–9
26. Kalamaras I, Daletou MK, Neophytides SG et al (2012) Thermal crosslinking of aromatic polyethers bearing pyridine groups for use as high temperature polymer electrolytes. J Membr Sci 415–416:42–50
27. Morfopoulou CI, Andreopoulou AK, Daletou MK et al (2013) Cross-linked high temperature polymer electrolytes through oxadiazole bond formation and their applications in HT PEM fuel cells. J Mater Chem A 1:1613–1622

28. Hsiao SH, Chiou JH (2001) Aromatic poly(1,3,4-oxadiazole)s and poly(amide-1,3,4-oxadiazole) s containing ether sulfone linkages. J Polym Sci A Polym Chem 39:2271–2286
29. Higashi F, Ogata SI, Aoki Y (1982) High-molecular-weight poly(*p*-phenyleneterephthalamide) by the direct polycondensation reaction with triphenyl phosphate. J Polym Sci Polym Chem Ed 20:2081–2087
30. Huisgen R, Sauer J, Sturm HJ (1958) Acylierung 5-substitutierter Tetrazole zu 1.3.4-Oxdiazolen. Angew Chem 70:272–273
31. Huisgen R, Sauer J, Sturm HJ et al (1960) Ringöffnungen der Azole, II. Die Bildung von 1.3.4-Oxdiazolen bei der Acylierung 5-substituierter Tetrazole. Chem Ber 93:2106–2124
32. Zaidi SMJ, Chen SF, Mikhailenko SD et al (2000) Proton conducting membranes based on polyoxadiazoles. J New Mater Electrochem Syst 3:27–32
33. Hibsham C, Cornelius CJ, Marand E (2003) The gas separation effects of annealing polyimide-organosilicate hybrid membranes. J Membr Sci 211:25–40
34. Wind JD, Bickel CS, Paul RD et al (2003) Solid-state covalent cross-linking of polyimide membranes for carbon dioxide plasticization reduction. Macromolecules 36:1882–1888
35. Matyjaszewski K (ed) (1996) Cationic polymerizations: mechanisms, synthesis, and applications. Marcel Dekker, New York
36. Daletou MK, Kallitsis JK, Voyatzis G et al (2009) The interaction of water vapors with H_3PO_4 imbibed electrolyte based on PBI/polysulfone copolymer blends. J Membr Sci 326:76–83
37. Daletou MK, Geormezi M, Vogli E et al (2014) The interaction of H_3PO_4 and steam with PBI and TPS polymeric membranes. A TGA and Raman study. J Mater Chem A 2:1117–1127
38. Bhatnagar A, Sharma PK, Kumar N (2011) A review on "Imidazoles": their chemistry and pharmacological potentials. Int J PharmTech Res 3:268–282
39. Ma YL, Wainright JS, Litt MH et al (2004) Conductivity of PBI membranes for high-temperature polymer electrolyte fuel cells. J Electrochem Soc 151: A8–A16
40. He R, Che Q, Sun B (2008) The acid doping behavior of polybenzimidazole membranes in phosphoric acid for proton exchange membrane fuel cells. Fiber Polym 9:679–684
41. Schechter A, Savinell RF (2002) Imidazole and 1-methyl imidazole in phosphoric acid doped polybenzimidazole, electrolyte for fuel cells. Solid State Ionics 147:181–187
42. Daletou MK, Kallitsis J, Neophytides S (2011) Materials, proton conductivity and electrocatalysis in high temperature PEM fuel cells. In: Vayenas C (ed) Interfacial phenomena in electrochemistry, vol 51, Modern aspects of electrochemistry. Springer, New York, pp 301–368
43. Wainright JS, Wang JT, Weng D et al (1995) Acid-doped polybenzimidazoles: a new polymer electrolyte. J Electrochem Soc 142:L121–L123
44. Samms SR, Wasmus S, Savinell RF (1996) Thermal stability of proton conducting acid doped polybenzimidazole in simulated fuel cell environments. J Electrochem Soc 143:1225–1232
45. Kreuer KD, Paddison SJ, Spohr E et al (2004) Transport in proton conductors for fuel-cell applications: simulations, elementary reactions and phenomenology. Chem Rev 104:4637–4678
46. He R, Li Q, Xiao G et al (2003) A study of water adsorption and desorption by a PBI-H_3PO_4 membrane electrode assembly. J Membr Sci 226:169–184
47. Lobato J, Cañizares P, Rodrigo M et al (2007) PBI-based polymer electrolyte membranes fuel cells: temperature effects on cell performance and catalyst stability. Electrochim Acta 52:3910–3920
48. Galbiati S, Baricci A, Casalegno A et al (2012) Experimental study of water transport in a polybenzimidazole-based high temperature PEMFC. Int J Hydrogen Energy 37:2462–2469
49. Li Q, He R, Jensen JO et al (2004) PBI-based polymer membranes for high temperature fuel cells—preparation, characterization and fuel cell demonstration. Fuel Cells 4:147–159
50. Gu T, Shimpalee S, Van Zee JW et al (2010) A study of water adsorption and desorption by a PBI-H_3PO_4 membrane electrode assembly. J Power Sources 195:8194–8197
51. Schmidt TJ, Baurmeister J (2008) Imidazole and 1-methyl imidazole in phosphoric acid doped polybenzimidazole, electrolyte for fuel cells. J Power Sources 176:428–434
52. Schechter A, Savinell RF, Wainright JS et al (2009) ^{1}H and ^{31}P NMR study of phosphoric acid-doped polybenzimidazole under controlled water activity. J Electrochem Soc 156:B283–B290
53. Li Q, He R, Berg RW et al (2004) A study of water adsorption and desorption by a PBI-H_3PO_4 membrane electrode assembly. Solid State Ionics 168:177–185
54. Li Q, Hjuler HA, Bjerrum NJ (2001) Phosphoric acid doped polybenzimidazole membranes: Physiochemical characterization and fuel cell applications. J Appl Electrochem 31:773–779
55. Lister S, McLean G (2004) PEM fuel cell electrodes. J Power Sources 130:61–76
56. Daletou MK, Paloukis F, Stefopoulos A (2009) Pt/modified MWNT as electrocatalysts for high temperature Fuel Cells. ECS Trans 25:1915–1924
57. Orfanidi A, Daletou MK, Neophytides S (2011) Preparation and characterization of Pt on modified multi-wall carbon nanotubes to be used as electrocatalysts

for high temperature fuel cell applications. Appl Catal B Environ 106:379–389
58. Orfanidi A, Daletou MK, Sygellou L et al (2013) The role of phosphoric acid in the anodic electrocatalytic layer in high temperature PEM fuel cells. J Appl Electrochem 43:1101–1116
59. Avgouropoulos G, Papavasiliou J, Daletou MK et al (2009) Reforming methanol to electricity in a high temperature PEM fuel cell. Appl Catal B Environ 90:628–632
60. Advanced Energy Technologies S.A.—Advent S.A. http://www.advent-energy.com/
61. Schmittinger W, Vahidi A (2008) Imidazole and 1-methyl imidazole in phosphoric acid doped polybenzimidazole, electrolyte for fuel cells. J Power Sources 180:1–14